Earth-Science Reviews 193 (2019) 317–332

Contents lists available at ScienceDirect

Earth-Science Reviews

journal homepage: www.elsevier.com/locate/earscirev

Chevrons: Origin and relevance for the reconstruction of past wind regimes

Lucas Vimpere*, Pascal Kindler, Sébastien Castelltort

Department of Earth Sciences, University of Geneva, Rue des Maraîchers 13, 1205 Geneva, Switzerland

ARTICLE INFO

Keywords:
Chevron
Climate change
Coastal risk
Tsunami
Storm wave
Dune
Eolianite

ABSTRACT

Since its first use in the late 80's, the term chevron has been employed in numerous studies to describe large U- and V-shaped ridges found in or near shorelines worldwide. Most studies have so far focused on Bahamian chevrons that are exclusively of Late Pleistocene age, and on the supposed Holocene chevrons found in S-Madagascar and Australia. In the Bahamas, these deposits have been interpreted as the product of extreme storms at the end of the last interglacial (LIG) warm period. In contrast, the extensive chevrons complex exposed in S-Madagascar and on the western coast of Australia have been associated with a tsunami induced by a meteorite impact. Finally, several authors have also proposed a non-catastrophic (i.e. eolian) origin based on the recognized importance of wind-related processes in these coastal areas, and term such deposits parabolic dunes. In this paper, we collect and synthesize existing data on the morphology, sedimentology and age of these chevrons, and review the different interpretations proposed in the literature with the aim to lay out a consistent database to assist further investigations on these important coastal morphologies. In addition, we generated a synthesis of wind data at the three study areas, which highlights the relationship between present wind regimes and chevrons morphologies. The ubiquity of chevrons (likely actually parabolic dunes) in coastal areas around the globe and their relationship with coastal processes makes them crucial archives for reconstructing past wind regimes.

1. Introduction

The term “chevron” is widely used to describe U- and V-shapes and has taken several descriptive usages in structural geology (e.g., chevron folds; Ramsay, 1974), and sedimentology (e.g., small-scale laminae arrangement in oscillatory ripples; Allen, 1982). Later, using Landsat MSS images at 80 m spatial resolution, Maxwell and Haynes (1989) mapped the 10′000 km^2 of the Selima Sand Sheet, SW Egypt (Fig. 1), where light-colored chevron-shaped patterns are observable migrating downwind over darker coarse sand. They described these features as active “extremely long-wavelength (130 to 1200 m) and low-amplitude (10 to 30 cm), […] irregularly spaced, light-toned, 0.5 to 2.0 km wide streaks oriented generally transverse to the dominant northerly wind direction […]” bedforms. By comparing Landsat images from 1972, 1986 and 1988, they defined a migration rate between 100 and 500 $m.y^{-1}$ corresponding to a net movement of 83′000 $m^3.y^{-1}$ of sand for a 10 km wide chevron. In the present review, we focus on the term “chevron” as it has been originally applied by these latter. Although the authors renamed them zibars thereafter (Maxwell and Haynes, 2001), the term was independently used for modern and Holocene coastal landforms of similar morphology in Australia (Bryant et al., 1997), and for Pleistocene ones in the Bahamas (Hearty et al., 1998).

Since their discovery, the origin of chevrons and their environmental significance have captured the attention of sedimentologists and geologists. Scheffers et al. (2008) characterized their morphology by using Google Earth© to identify 221 chevron sites along the world coastlines (Fig. 1). To qualify as a chevron, the distinctive U to V-shape was used as the diagnostic criterion. They found that the common extension of a chevron field is between 10 and 50 km (49% of their data), making such bedforms very significant sediment transport systems. Furthermore, 61% of the identified chevrons have a kilometric lateral extension (length: 1 to 5 km, width: 10 to 1000s m), and 59% of them display an elevation between 10 and 100 m a.s.l. The main characteristic of these bedforms is the linearity of their axes despite the different morphologies they exhibit (Fig. 2). Five different chevron morphologies have been categorized, lying the foundations for a more complete classification, subsequently defined by the same authors.

Both of these systematizations are similar to the one proposed by Pye (1993) in his study of parabolic dunes in Queensland, NE-Australia, which is based on the architecture and the length/width ratio (Fig. 2). Using the classification presented by McKee (1979), the morphology of dunes is subdivided in three categories: *simple*, *compound* and *complex*.

* Corresponding author.
E-mail address: Lucas.Vimpere@unige.ch (L. Vimpere).

https://doi.org/10.1016/j.earscirev.2019.04.005
Received 19 December 2018; Received in revised form 2 April 2019; Accepted 5 April 2019
Available online 16 April 2019
0012-8252/

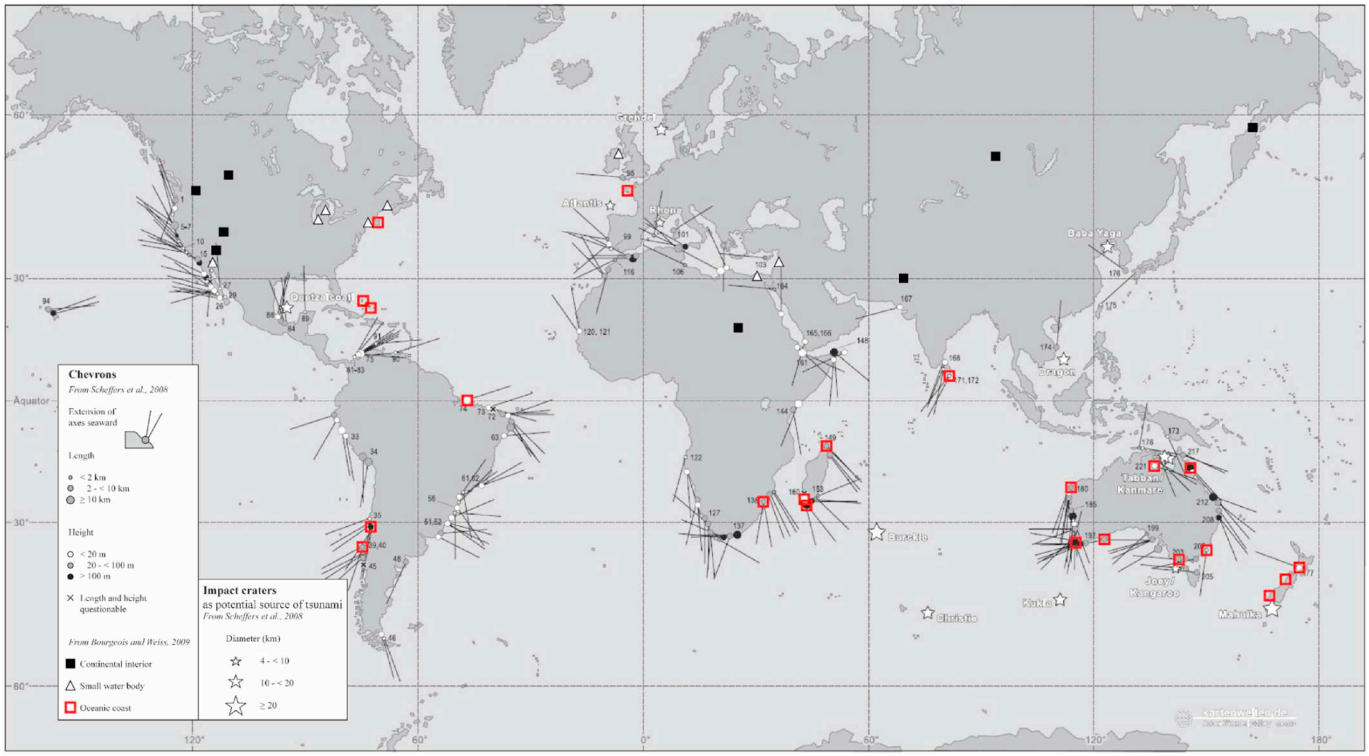

Fig. 1. World map of chevron distribution along coasts and their approximate seaward axes, pointing to a potential source area (modified after Scheffers et al., 2008). The stars show the impact craters defined by those authors. Squares and triangles point the approximate locations of chevrons and/or parabolic dunes observed by (Bourgeois and Weiss, 2009). The authors defined three categories of bedforms according to their relationship to a coastline: "'interior' cases have no relationship to a coastline (black squares); 'small water body' cases require improbable impact scenarios (triangles); for 'oceanic coast' cases, impact hypothesis requires further evaluation (red squares)". Depending on the authors and the proposed interpretation, the number of chevrons and the associated localities change. (For interpretation of the references to colour in this figure legend, the reader is referred to the web version of this article.)

Simple dunes are characterized by single forms subclassified by Pye (1993) as *lunate* when they exhibit length:width (L/W) ratio < 0.4; *hemicyclic* for 0.4 < L/W < 1.0; *lobate* when 1.0 < L/W < 3.0 and *elongate* for those with a L/W > 3.0. Compound forms consist of two or more dunes of the same type that have coalesced or are superimposed, and complex dunes are composed by two or more different types of simple dunes.

Some authors suggested a tsunamigenic origin for the chevrons from S-Madagascar and W-Australia (Abbott et al., 2005; Abbott, 2006; Abbott et al., 2006, 2007, 2010a, 2010b; Bryant and Nott, 2001; Gusiakov et al., 2009; Kelletat and Scheffers, 2003; Masse et al., 2006; Masse, 2007). Others proposed that Bahamian chevrons result from the action of large waves generated during "superstorms" (Hansen et al., 2015; Hearty et al., 2002, 1998; Hearty and Tormey 2018a, 2018b, 2017; Tormey and Donovan, 2015). Finally, several authors proposed a non-catastrophic, wind-induced origin for the chevrons in the three mentioned regions (Bourgeois and Weiss, 2009; Engel et al., 2015; Kindler and Strasser, 2002, 2000; Mylroie, 2018a, 2018b; Pinter and Ishman, 2008; Rovere et al., 2018, 2017). These Eolian deposits are regarded by these authors as parabolic dunes, not chevrons.

Determining whether chevrons result from giant-storm waves, asteroid- or landslide-related tsunamis or eolian processes has important implications for the assessment of coastal hazards, landscape and infrastructure management in these regions and for the correct interpretation of genesis of coastal and near-coastal landforms, especially in the current context of climate change and sea-level rise. It is beyond the scope of this paper to present scenarios of possible coastal evolution associated with the ongoing global warming. However, research on the origin of chevrons from the Bahamas, in relation with the LIG climatic optimum, may provide "facts from the past" and a perspective of the possible consequences of the current temperature trend. In addition, although the LIG may not be a perfect analogue for present climate change, it represent an important case of a ***natural*** increase of greenhouse gas concentration in the atmosphere (Hansen et al., 2015, 2013; Masson-Delmotte et al., 2013; O'Leary et al., 2013), thereby providing a benchmark against which the impact of the anthropogenic addition of such gases to the atmosphere may be gauged.

In addition, because coastal chevrons are recognized in recent settings due to their plan-view shape, they may have been overlooked in ancient sedimentary successions. Understanding how chevrons originated could thus improve our ability to quantify past environmental conditions and extreme events that have affected coastal regions.

The objectives of this paper are thus to synthesize existing knowledge on the morphology, sedimentology, age and depositional processes of these landforms.

2. The Bahamas

2.1. Morphology

In the Bahamas, chevrons are found across the archipelago but are concentrated in its northern and central part. They are exclusively located on the coast facing the Atlantic Ocean. They can be composed of multiple smaller ridges in nested sets that extend several kilometers across several islands, with asymmetrical SW-pointing seaward-dipping crests (Hearty et al., 1998; Hearty and Tormey, 2017).

2.2. Sedimentology

As most deposits from the last interglacial (i.e. MIS 5e), apart from reefal complexes, chevron ridges display an oolitic composition with a subordinate skeletal content (Hearty et al., 1998; Kindler and Hearty,

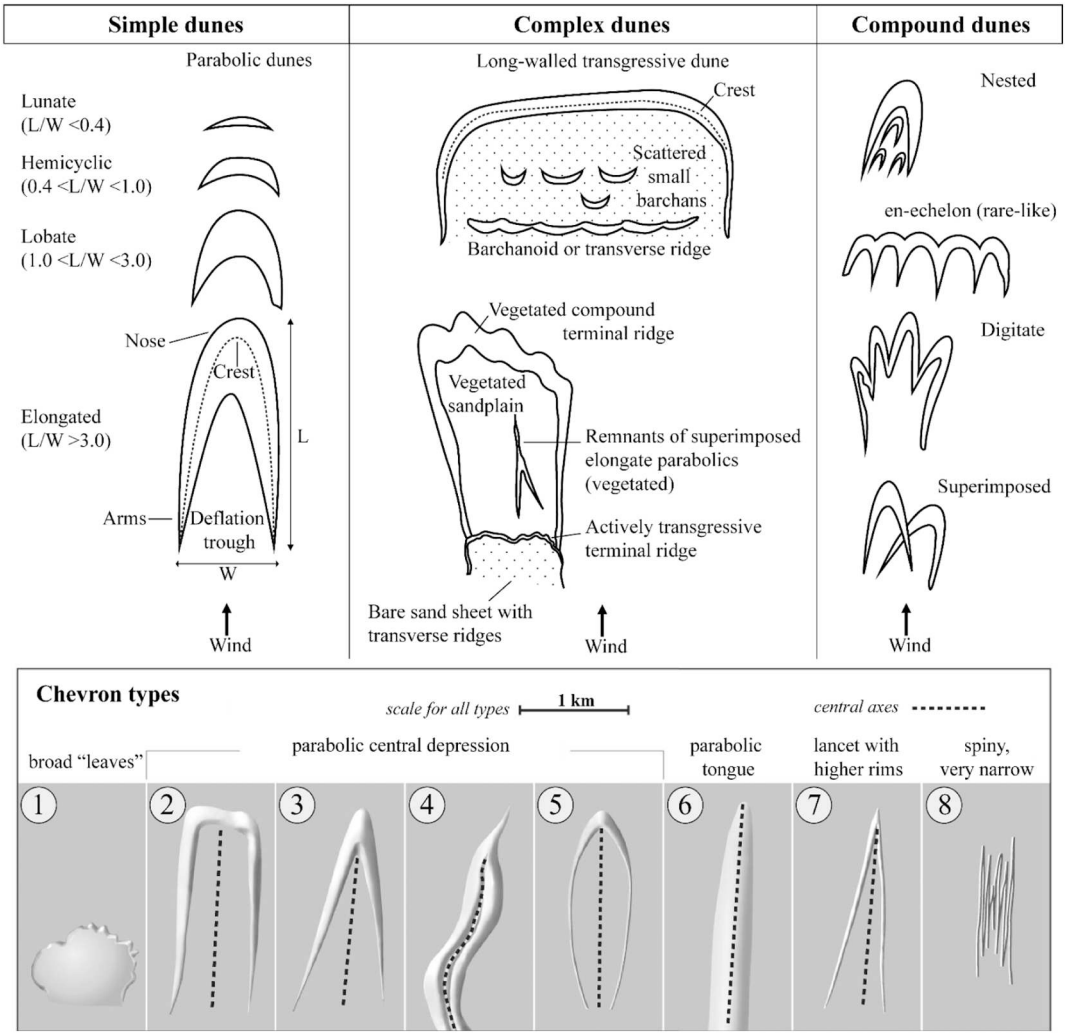

Fig. 2. The three types of dunes defined by McKee (1979) and the subclassification of sample dunes according to their length:width ratio (Pye, 1993). Comparison with the eight types of chevron morphology observable around the world (modified after Scheffers et al., 2008).

1996). Hearty et al. (1998) described the chevron's sedimentary features as: "[…] subparallel, aggrading beds with few interruptions or truncations". It was later emphasized that steep foresets are absent in Bahamian chevrons, and that pedogenic features as well as eolian strata are rare (Hearty and Tormey, 2017). Thin (5 to 20 cm thick) fenestrae-rich beds have also been observed within chevrons and coastal ridges oriented parallel to the coastline (Bain and Kindler, 1994; Hearty et al., 2002; Hearty and Tormey, 2017; Kindler, 1991; Kindler and Strasser, 2002, 2000). Detailed descriptions of exposures from several localities on different Bahamian islands have resulted in the definition of three types of fenestral beds changing with elevation and distance from the shore (Hearty and Tormey, 2017; Tormey and Donovan, 2015). From the lowest and most proximal to the highest and most distal locations, fenestral beds are respectively unlaminated, abundant and tabular, and end up forming slight, discontinuous packages. Intermediate morphologies can be observed at moderately elevated and inland positions (Fig. 3). Last but not least, mm-thin, inversely graded laminae, identified as SCTS (Hunter, 1977) and outcropping as "pin-stripe laminations" Fryberger and Schenk (1988) have been observed in the chevrons (Kindler and Strasser, 2002, 2000).

2.3. Geochronology

In the Bahamas, the most widely used dating method is amino-acid racemization (AAR) geochronology, which consists in measuring the ratio between alloisoleucine and isoleucine (A/I) in shells or whole-rock samples. U/Th-calibrated A/I measurements on whole-rock samples yield a ratio of 0.48 ± 0.04 for the first part of the last interglacial (MIS 5e), and 0.40 ± 0.03 for the later portion of this substage (Hearty and Kaufman, 2009, 2000). Only one chevron located in Miller's Settlement on Long Island has been directly dated by AAR. The authors obtained two A/I ratios averaging at 0.46 (Appendix 1), and correlated the chevron to the late Pleistocene (Aminozone E; MIS 5e II; Hearty and Kaufman, 2000). The other ridges are correlated to the latter based on their petrography, stratigraphic position and dating of associated deposits such as mega boulders or runup deposits (Hearty et al., 2002, 1998; Hearty and Tormey, 2017; Kindler, 1991; Kindler and Strasser, 2000).

3. Australia

3.1. Morphology

Based on aerial photographs investigation in Australia, and particularly in W-Australia, chevrons show a very extended distribution around the country and different morphological appearances (Kelletat and Scheffers, 2003). These authors observed similar ranges of sizes, field extensions and nesting as in the Bahamas. The ridges are one to several kilometers in length, heights of 10 m to > 120 m. They usually have straight axis that may be perpendicular, parallel or oblique to the

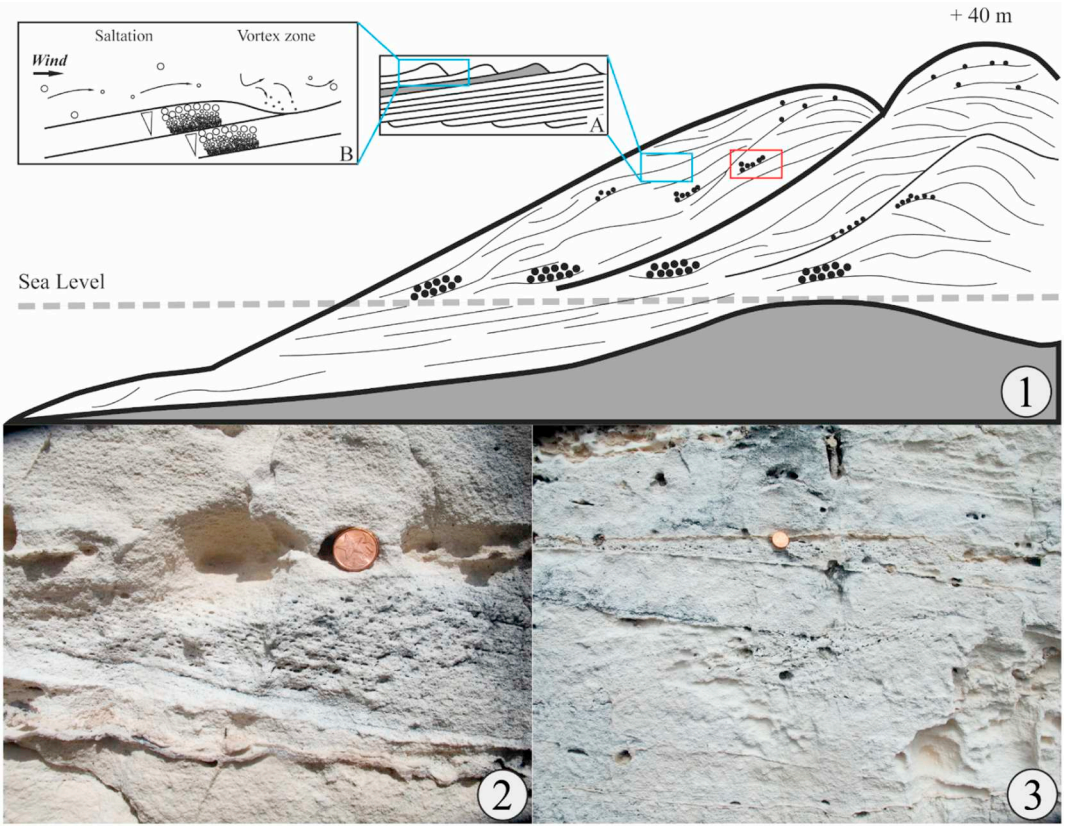

Fig. 3. 1—Changing morphology of fenestrae-rich beds within chevron dunes, going from abundant tabular to slight discontinuous packages with increasing distance and elevation from shore (modified after (Hearty and Tormey, 2017). Red square indicates the position of 2 and 3. A— Subcritically translatent strata (SCTS) forming when the angle of ripple climb is lower than the inclination of ripple stoss slope (modified after Hunter, 1977). B—Formation mechanism of pine stripe laminations showing inverse grain size gradient by concentration of finer particles in the existing trough between two ripples (modified after (Fryberger and Schenk, 1988). 2 and 3—Photographs of fenestrae-rich beds of a dozen cm thick within an eolianite subparallel to the coast. Note the more pronounced pinstripe laminations within the bed rich in fenestrae in 2. (For interpretation of the references to colour in this figure legend, the reader is referred to the web version of this article.)

coast, but can sometimes bend in two directions with a 90° shift. They described landward-narrowing, sharply marked outer contours, often covered by vegetation and soil even in the dry bush. At least two generations were defined according to their degree of erosion and vegetation cover. Active beaches act as sources of sediment, but chevrons also developed at locations where there is no apparent source of sand. However, each of the studied location has been the subject of a previous publication in the literature, describing climbing and clifftop dunes all along the Australian coast, including parabolic ones (Hesp and Chape, 1984; Short, 2014, 2006, 2005, 1988; Woodroffe, 2002). Jennings (1967) postulated that cliff-top dunes imply cliff recession or erosion of a sand ramp after the deposition. Since sand can be blown up slopes up to 60° (Pye and Tsoar, 2008), and deposited in the zone of reduced wind velocity near the crest of escarpments (Bowen and Lindley, 1977; Jackson, 1975; Marsh and Marsh, 1987), cliff-top dunes do not require a nearby source, nor a change in sea-level or tectonic regime. (Kelletat and Scheffers, 2003) also studied Cape Melville area, located on the coast of Queensland, NE-Australia, where they observed two different generations of inactive ridges, interpreted as chevrons. Again, previous work (Jennings, 1957; Lees et al., 1990; Pye, 1993, 1983, 1982a, 1982b; Pye and Mazzullo, 1994; Pye and Rhodes, 1985; Short, 2014 1988; Shulmeister and Lees, 1992; Tejan-Kella et al., 1990; Ward, 2006) interpreted variations in **parabolic dune** morphology all along the Queensland coast as the result of changes in wind regime, local topography, sand availability and vegetation.

3.2. Sedimentology

All studies performed on the chevron ridges from Australia mostly consist of geomorphic descriptions based on aerial photographs and/or field observations, but no thorough sedimentological or petrographic study has been conducted yet. However, the sedimentology of parabolic coastal dunes in Queensland (later named chevrons by (Kelletat and Scheffers, 2003; Scheffers et al., 2008) has been studied before the use of the term “chevron” became widespread (Pye, 1993). Drilling data demonstrate a long history of coastal dune building in this region with several generations of deposits, separated by soil horizons with different degrees of pedogenesis, that extend > 40 m below the surface. Eolian deposits supposedly accumulated during both highstand and lowstand periods. The Holocene marine transgression, and probably earlier ones, have trimmed sandy coastlines and provided the material for dunes to migrate landward from these eroding shorelines. The migration coupled with a partial stabilization yielded to the formation of parabolic dunes or chevrons of large size. Chevrons have nonetheless been described on the southern headland of Jervis Bay where they form two lines of deposits, respectively lying at + 30 and + 130 m a.s.l., and consisting of sand mixed with cobbles and fine shell hash (Bryant et al., 1997; Bryant and Nott, 2001).

3.3. Geochronology

Using ^{14}C dating on various deposits attributed to tsunamis, including chevron dunes, Bryant and Nott (2001) obtained Holocene ages from 0 to almost 7 ka BP. Kelletat and Scheffers (2003) briefly mentioned that chevrons have been dated (1) at around 123′000 ± 5000 BP without specifying the location, and (2) at 1080 CE in at least one place in W-Australia, but again without referencing their source. They mostly interpreted chevrons as Holocene deposits because of their

relation to active coastline, with an older Holocene age shown by their basal erosion by beach ridges. Later, relative age indicators such as the density of the vegetation cover, the sharpness of contours, the co-existence of several generations of ridges and their relationships to the modern coast have been used based on satellite images (Scheffers et al., 2008). The coast of Queensland is far better known as stratigraphic studies have been conducted along several zones (Lees et al., 1990; Pye, 1993; Pye and Switsur, 1981). The petrographic and diagenetic analyses coupled with ^{14}C and TL ages, when reassembled, define a stratigraphic column composed of seven units named from A to G (from top to bottom). The oldest observed record of eolian activity in this region was dated from middle Pleistocene (Appendix 1).

4. Madagascar

4.1. Morphology

A complete study has been conducted in the southern part of Madagascar to investigate its geomorphological components and define a stratigraphic column (Battistini, 1964). The Ampalaza "chevron" has been defined by the author as linguiform complexes of parabolic dunes whereas the Fenambosy "chevron" combines fixed parabolic and active transverse dunes. Battistini (1964) recognized three sub-complexes within the Ampalaza dunefield (Fig. 4):

1) The first linguiform field is the oldest and innermost one. The ridges composing it are altered by the erosion and entirely covered by the vegetation.
2) The second and most extended one corresponds to an intermediate progradation phase. With a length of about 30 km and a width of 2.5 to 4 km, it composes 30% of the chevron. Fixed by the vegetation for the most part, it overlies older sandstones to reach an altitude of 77 m.a.s.l. Only the NW extremity is still active and migrates according to the general orientation.
3) Between the second sub-complex and the sea, the third phase of progradation consists on active bare sand that overlies the dunes of the second phase in some places. It is 2 to 4 km wide and 18 km long.

Regarding the Fenambosy dunefield, five phases have been defined (Fig. 4):

1) The youngest one is an active foredune coming from the beach with numerous deflation zones and nebkhas.
2) A second one on the eastern part of the field, composed of active bare sand migrating as transverse dunes that overlie older fixed parabolic dunes in the innermost part.
3) A middle part very extended and covered by the vegetation. It strictly consists of parabolic dunes that can be more or less elongated.
4) A migrating inner part 12 km long and 2 to 2.5 km wide that reaches the altitude maxima. Some large parabolic dunes (about 15) show active bare sand migrating NW and the associated deflation zones where nebkhas may develop. A transition to transverse dunes can be observed landward where the absence of vegetation allows a rapid migration of the ridges.
5) NE of the fresh active linguiform complex, an older phase of sand migration displays smoothed reliefs. The ridges, now partially eroded, climbed up the fault escarpment to reach an altitude of 211 m.a.s.l.

Chevrons from S-Madagascar have been morphologically compared to those described in the Bahamas and Australia, and to subaqueous dunes and ripples in the Palouse region, E-Washington State, using a sedimentological approach (Bourgeois and Weiss, 2009). These authors concluded that chevron grain diameter (D), length (L), height (H), L/H and L/D ratios are highly similar in all the studied regions (Table 1; Bahamian chevrons slightly differ from the others but have the same order of magnitude). Unlike the rather isolated chevrons in the Bahamas than can be found nested, and the large complex extending along the Australian coastlines, the chevrons in Madagascar form massive linguiform complexes of dunes (Fig. 5). Later, other authors used and described the mentioned ridge complexes as parabolic dune fields (Hesp, 2011, p. 2011; Hesp and Walker, 2013).

4.2. Sedimentology

The source of sediment for the Fenambosy chevron is the eastern

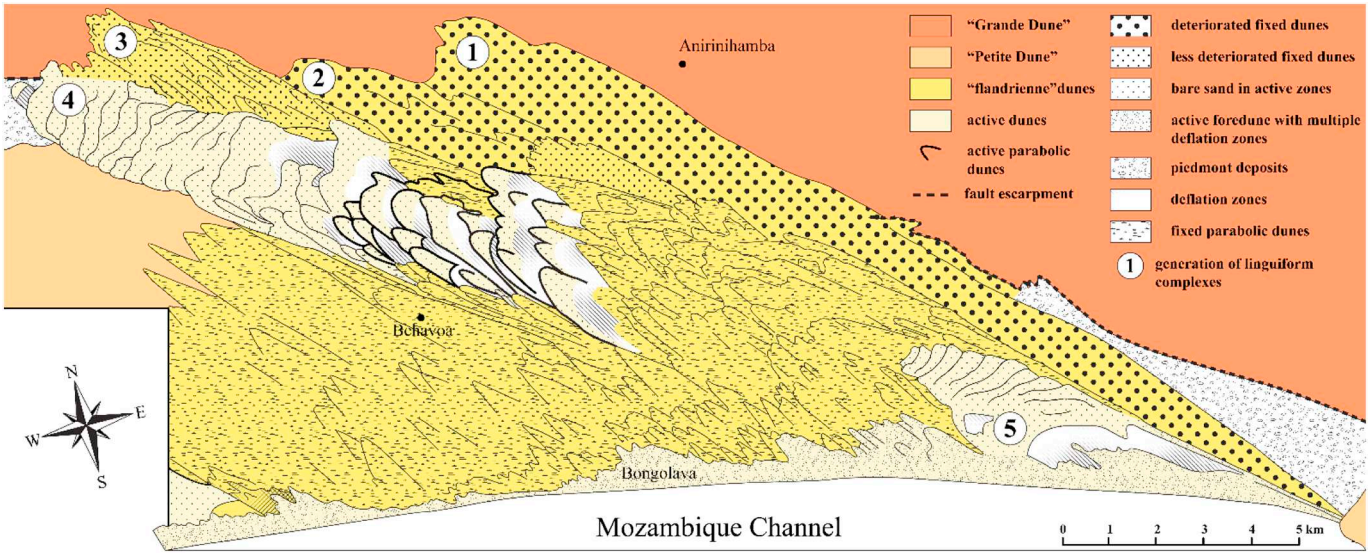

Fig. 4. Geomorphological features and stratigraphic relationships of the different units composing the Fenambosy chevron (modified after Battistini, 1964). The "Grande Dune" is the oldest sandy unit in S-Madagascar coastline environment, correlated to the ancient "Aepyornien" (from 2.2 Myrs to 160′000 yrs. BP). The "Petite Dune" unit corresponds to the "karimbolien" deposits (120′000–45′000 yrs. BP). The "flandrienne" dunes are Holocene (6′000 yrs. BP) transgression-related sandy deposits that form the chevrons in the region. The active recent dunes are depositing as foredunes on which few nebkhas can be observed. The numbers represent the different phases of deposition from the oldest (generation 1) to the youngest (generation 5).

Table 1
Comparison of some bedform characteristics measured for chevrons around the globe and other common bedforms (Bourgeois and Weiss, 2009).

	Grain diameter, D (m)	Bedform length, L (km)	Bedform height, H (m)	L/H (m/m)	L/D (m/m) × 10^4
Subaqueous sand ripples, typical	0.00015	0.00015	0.01	15	0.1
Subaqueous sand dunes, typical	0.00015	0.015	1	20	10
Washington State giant ripples	0.02–0.3	0.04–0.1	1–5	20	≈0.03–0.2
Washington State parabolic dunes	≈0.001	≈0.3	≈3	≈100	≈25
Oolite chevrons, Bahamas[a]	0.002	3–10[a]	8–25	≈400	150–500
Australia "chevrons"	0.002	0.5–3	≈3–30[b]	≈100–200	25–150
Madagascar "chevrons"	0.002	0.5–3	≈3–30[b]	≈100–200	25–150

[a] Not regularly repeating.
[b] Estimates based on general characteristics in literature.

part of the active beach. This 10 km long zone is located between Malaimpioka Cape and the locality Bongolava. Battistini (1964) suggested that longshore drift towards the West accumulates sediments on this beach because the presence of a steep rocky cliff in the West. Being more resistant to the erosion, it induces a local low sediment supply. The active front part (generation 4; Fig. 4) is still migrating fast but is already disconnected from the littoral source by the fixation of the parabolic dunes. As a result, a new generation of dunes (generation 5; Fig. 4) is migrating from the beach on the vegetated parabolic dunes. The Menrandra mouth is located to the West of the Ampalaza chevron and acts as the main source of sediment. The associated lagoon is reformed each year during the dry season.

4.3. Geochronology

According to the stratigraphy defined by Battistini (1964), all chevrons in S-Madagascar are correlated to the "flandrienne" transgression that occurred around 6′000 yrs. BP. They now partially cover the older "Petite Dune" unit correlated to the "karimbolien" high sea-level (120′000 to 80′000 yrs. BP), which roughly corresponds to the Eemian or LIG. During the Holocene transgression, a dense psammophile vegetation that partly fixed the migrating bare sand, inducing the formation of parabolic dunes (Lebigre et al., 2001). The stratigraphic relationships between the different units are summarized in Fig. 4 for the Fenambosy chevron, and in Appendix 2 for the Ampalaza chevron.

Radiocarbon-dated archeological discoveries (Blench, 2010; Burney

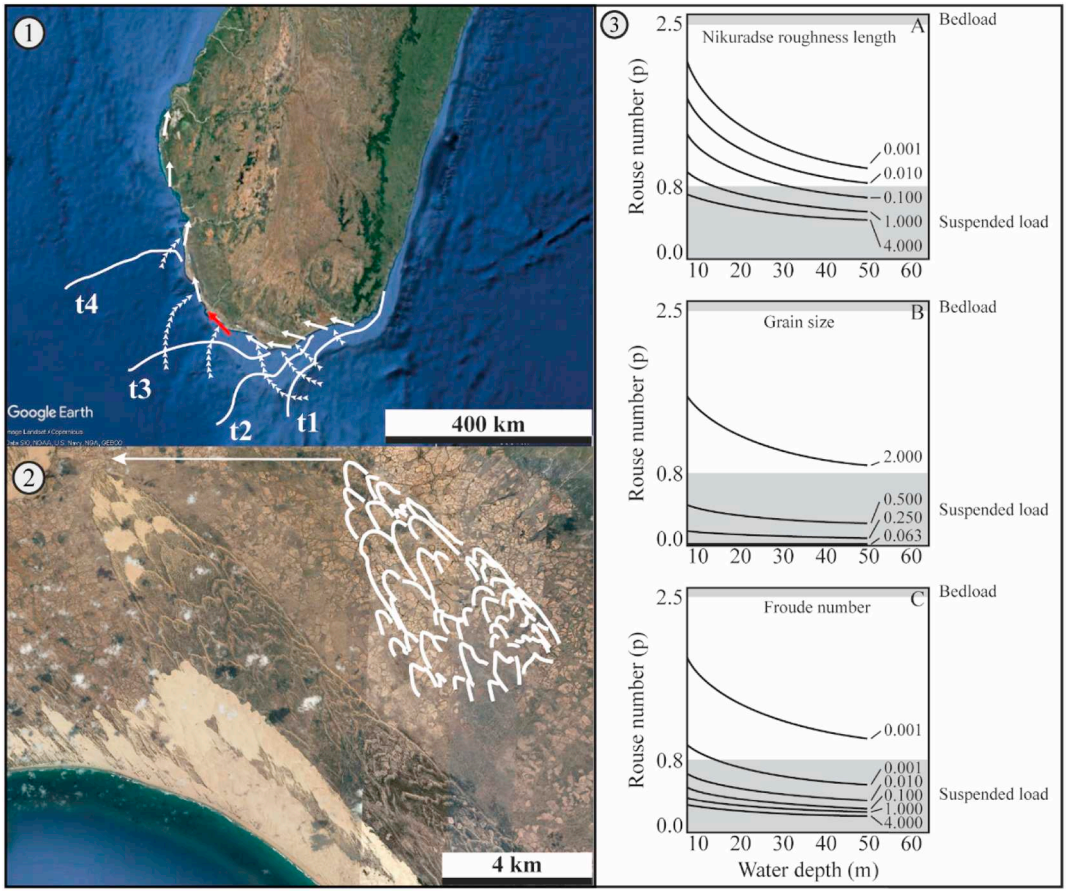

Fig. 5. 1— Satellite photograph of the southern part of Madagascar. The arrows show the chevrons orientations, and specifically the Ampalaza chevron (red arrow). The timelines of wave crests modeled by Bourgeois and Weiss (2009) are represented by the uniform white lines, and angles of wave approach by arrowed ones. 2— Enhancement of the Ampalaza chevron with the main ridges outlined in white (Bourgeois and Weiss, 2009), showing the general orientation subparallel to the coast. 3— Plots of Rouse number (p) versus water depth to show the type of sediment transport under varying k_s (A), D (B) and *Fr* (C) represented by the lines (Bourgeois and Weiss, 2009). Grain size is kept constant (D = 1 mm) in A for all cases; as *Fr* = 1.0 and k_s = 1 m in B; plus D = 1 mm and k_s = 1 m in C. (For interpretation of the references to colour in this figure legend, the reader is referred to the web version of this article.)

et al., 2004), coupled with the presence or absence of oral history in S-Madagascar, made it possible to approximately constrain the chevron maximum age at ca. 500 CE (Gusiakov et al., 2009). Based on the general appearance and vegetation cover, a mid-Holocene age (7′000–4′000 years) was proposed. The authors suggest that because there are fragile, unconsolidated features, chevrons would not have been preserved after the Younger Dryas climatic change.

Older detailed studies conducted in the region correlate the chevrons to the "post-karimbolien" period that occurred between 120′000 and 45′000 (Battistini, 1964; Lebigre et al., 2001).

5. Emplacement mechanisms

5.1. Giant storm wave hypothesis

Building up on an hypothesis formulated by Hearty et al. (1998), and integrating recent assessments on the LIG climate (DeConto and Pollard, 2016; Engel et al., 2015; Hansen et al., 2015, 2013; Hearty et al., 2007; Kopp et al., 2009; O'Leary et al., 2013), Hearty and Tormey (2017) reiterated the giant-wave theory for the formation of chevrons in the Bahamas. There, chevrons are associated with large boulders and runup sediments, thereby seemingly constituting a "trilogy" of long-period wave deposits (Hearty et al., 2002, 1998; Hearty and Tormey, 2017). Chevrons were accumulated in lowlands delineated by older ridges, the lower portions of which were potentially the source of the large boulders, whereas sand sheets were deposited over the ridges by wave runup (Fig. 6).

This trilogy can be observed in North Eleuthera, near the Glass Window bridge, where chevrons occur close to megaboulders and runup deposits. Seven boulders with a volume ranging from 500 to 1000 m^3, and weighting from about 300 to 2000 tons lie in the vicinity of the bridge (Hearty, 1997). Evidences for their erratic origin consist of high-angle bedding (30° to 75°; Hearty and Tormey, 2017) and their stratigraphic position above younger units. Because no major tsunami struck the Bahamian coastlines in historical times, the storm-wave hypothesis appeared as the most plausible one. The authors referred to a

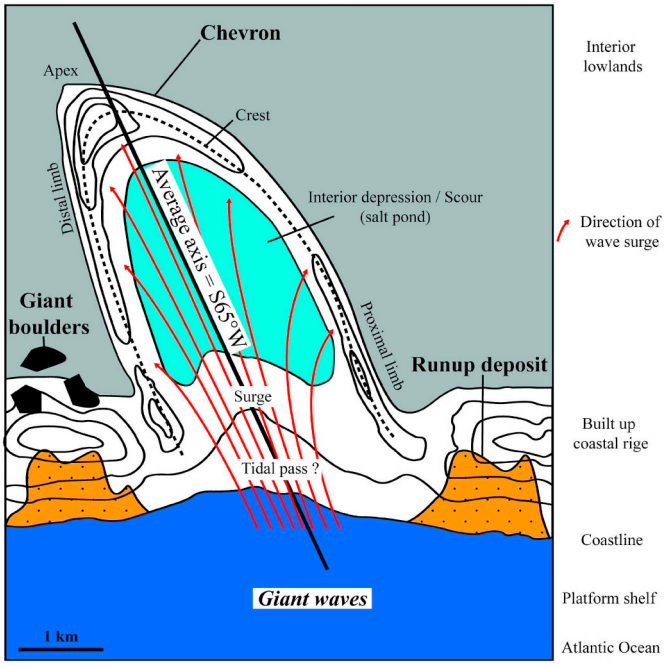

Fig. 6. Schematic map of a chevron, associated giant boulders landward of highlands and runup deposits on older built up ridges, following the impact of a giant wave coming from the Northern Atlantic Ocean (modified after Hearty et al., 1998).

"diminutive analogue", called "Perfect Storm" that generated a wave responsible for the horizontal displacement of the GW bridge weighting 510 tons. The natural rock bridge painted by Winslow Homer in 1895 was also washed away by storm waves (*https://www.eleuthera-map.com/rage-glass-window-bridge-1.htm*).

Runup deposits observed near chevron dunes are composed of stacked sequences of tabular, seaward-dipping beds showing fenestrae-rich levels. The composition is the same as chevrons and consist of a well-sorted oolitic grainstone. They can be associated with scour structures and rip-up breccia in some places, advocating for the erosive power of storm waves runup (Hearty et al., 1998; Hearty and Tormey, 2017; Tormey and Donovan, 2015). Furthermore, the changing character (scarcity and continuity) of fenestral beds within chevrons and runup deposits appears to reflect an attenuation of large waves on coastlines (Hearty and Tormey, 2017; Tormey and Donovan, 2015).

The LIG sea level history remains moderately well understood despite the numerous studies conducted (see Hansen et al., 2015 for a review of past studies). Climatic transitions between glacial and interglacial periods are strongly affected by insolation change (Hays et al., 1976), as it drives the growth and decay of Northern Hemisphere ice sheets. The warm-season insolation anomalies were negative during the MIS 5e, which was supposed to trigger the decay of ice sheets. To answer this paradox, several studies proposed that East and West Antarctic ice sheets and basins collapsed during this period, resulting in an abrupt sea level rise (DeConto and Pollard, 2016; Hansen et al., 2015; Hollin, 1965; Mercer, 1978; Neumann and Hearty, 1996; Wilson, 1964). For Hansen et al. (2015), the injection of fresh melt water in the Atlantic has dramatically increased the pressure gradient at the surface, strengthening northeasterly winds that would have contributed to the generation of long-period waves, amplified thereafter by local coastal bathymetry, reflection and refraction (Hearty and Tormey, 2017).

5.2. Cosmogenic tsunami hypothesis

In Australia, most of the chevrons have been correlated to the Holocene (cf. Chap. 3.3), enabling some authors to cross-check the geological imprint of tsunamis with oral traditions and mythologies (Bryant et al., 2007; Masse, 2007; Masse and Masse, 2007). Several studies mention the impact of past intense tsunamis on Australian coastlines, especially on the west coast (Bryant, 2014; Gusiakov et al., 2009). Imbricated boulder fields located onshore, in particular along the East coast (Bryant, 2014; Gusiakov et al., 2009), evoke the concrete block that was moved 150 m from the coastline during the Japan tsunami of 1983 (Gusiakov et al., 2009). Because chevrons orientation does not necessarily coincide with the dominant wind direction, and their limits occur far above any deposits of recorded storms or seismogenic and volcanic tsunamis, a cosmogenic impact was suggested as a probable formation process (Abbott, 2006; Abbott et al., 2007; Bryant, 2014; Gusiakov et al., 2009; Kelletat and Scheffers, 2003; Masse, 2007; Scheffers et al., 2008). Another argument was the presence of chevron fields along cliffed coasts where a source of available sediment is absent (Scheffers et al., 2008), and the extent of these complexes, especially on the South-Madagascar coast where they climbed the major fault escarpment reaching heights of > 200 m.a.s.l with inland penetration about 45 km (Gusiakov et al., 2009).

By extending chevrons orientations, Kelletat and Scheffers (2003) predicted an impact zone in the Indian Ocean at the same latitude as Perth. The large Burckle crater (29 km in diameter) was then discovered and related to the Madagascar and W-Australia chevrons (see Gusiakov et al., 2009 for a review of past studies). Because of its subtle morphology, the authors are certain that the crater cannot be interpreted as a submarine volcano, which usually have a more pronounced relief, or as a fault-block basin, that do not adopt a circular shape even within the Southwest Indian Ridge. Deep cores taken in the crater area revealed impact ejecta, of which the most diagnostic ones are: 1) melted droplets of NiO at the base of pure Ni grains, 2) nearly pure carbon spherules,

and 3) calcite rhombohedrons at a depth where ocean waters are undersaturated with respect to calcite (Abbott et al., 2005; Gusiakov et al., 2009). The ages obtained for chevrons (cf. Chap. 4.3) were correlated to the estimated Holocene age (4′500 to 5′000 y BP) of the Burckle impact crater located in the S-Indian Ocean (Abbott, 2006; Abbott et al., 2007, 2006; Gusiakov et al., 2009; Kelletat and Scheffers, 2003; Masse, 2007; Masse et al., 2006; Scheffers et al., 2008; Scheffers and Kelletat, 2003).

5.3. Eolian hypothesis

In the Bahamas, a few studies argued that fenestral porosity does not only occur in intertidal environments (Bain and Kindler, 1994; Kindler, 1991; Kindler and Strasser, 2002, 2000), implying their occurrence in chevrons may not be necessarily related to large waves. High-elevation fenestrae have been observed in eolianites of early MIS 5e, middle Pleistocene, and Holocene age in the Bahamas (Engel et al., 2015), which disagrees with Hearty et al. (1998) who restricted these features to the late MIS 5e chevrons and runup deposits. Stieglitz and Inden (1969) had already interpreted fenestrae within a spillway as the results of heavy rains. Moreover, Kindler and Strasser (2002, 2000) observed pin-stripe laminations in the run-up deposits and chevron ridges, and argued that such extensive, mm-thin lamina with an erosive base, that show an inverse grain-size grading in well-sorted sands devoid of gravel-size debris of marine origin, are typical eolian features. They further agreed that backwash-generated, low-angle cross-strata can also display inverse grain-size grading, but at a larger scale (1–2 cm thick) and are not as extensive. In addition, they reasoned that chevron morphology does not correspond to that of washover fans (Fig. 7), which exhibit landward dipping plane beds (Schwartz, 1982), and point in a downwind direction paralleling the axes of the northeasterlies that constantly blow the Atlantic coast of the Bahamas (Kindler and Strasser, 2000).

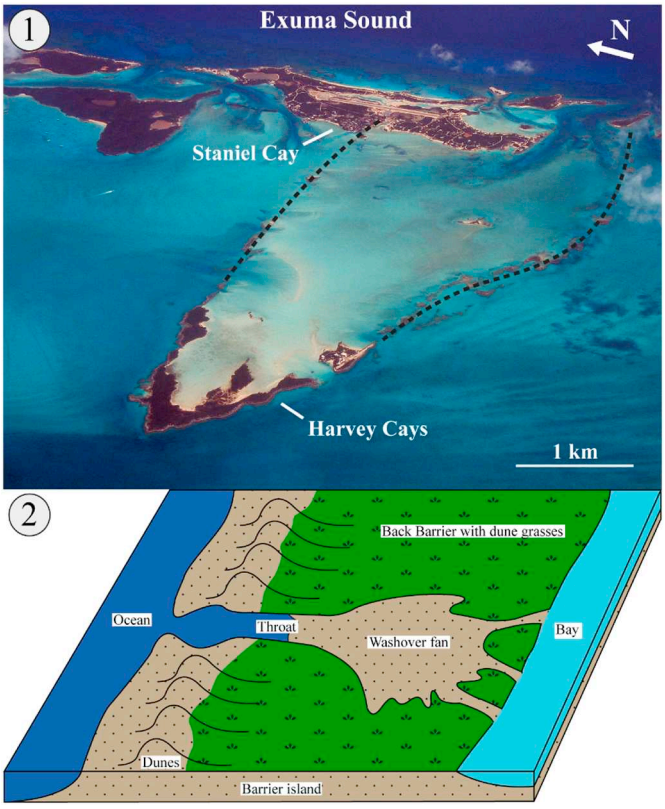

Fig. 7. 1— Aerial photograph of a partially eroded chevron near Staniel Cay in the Exumas, Bahamas (photo from P. Kindler). 2— Comparison with a typical washover fan morphology on a barrier island (modified after Donnelly et al., 2006).

The more complete sedimentological assessment of Malagasy chevrons by Bourgeois and Weiss (2009) and their comparison with the Palouse parabolic dunes suggest a similar formation process for both bedforms (Table 1). Their measurements of bedform characteristics show two distinct ranges for subaqueous and eolian deposits. They added that features similar to chevrons are common in continental interiors, sometimes related to bodies of water. They also modeled the wave approach pattern and compared it to the orientations of chevrons along the Malagasy coast (Fig. 5). Considering a small impact in deep water and the regional bathymetry, the resultant refraction and reflection involved when potential tsunamis approach the S-Madagascar coastline are not aligned with chevron orientations. The wave crests would have been parallel to the shore and with a perpendicular approach to it. Finally, they modeled the transport conditions occurring in a flow able to deposit a chevron. They have listed several factors influencing basic bedforms characteristics (L and H): settling velocity, shear stress, flow depth, bed erodibility (e.g., vegetation) and roughness (k_s), sediment supply, flow structure and grain size (D). They defined dunes as features scaled by excursion length of grains, where sediment availability and flow depth (h) are the limiting factors of growth with a ratio of $H < 0.5\,h$. Given that the majority of chevrons have an elevation between 10 and 100 m.a.s.l (Scheffers et al., 2008); the minimum flow required would have reached > 200 m.a.s.l.. Moreover, the Rouse number (p) is an indicator of the type of transport adopted by particles under specific flow conditions. When it exceeds 2.5, bedload transport prevails, whereas when it is inferior to 0.8, only suspension load conditions occur and so the wash out of the bedform (Shen and Julien, 1993). This dimensionless number is a relationship between grain settling velocity (w_s), shear velocity (u_*) and the von Kármán constant (Vanoni, 1975; Yalin, 1977). By examining p and h under varying k_s, D and Froude number (*Fr*), none of the modeled configuration generates pure bedload transport resulting in an instability of the bedform (Fig. 5). Therefore, they concluded by rejecting the tsunami hypothesis and by defining the chevrons in Madagascar as parabolic dunes.

5.4. Associated deposits

Concerning the megaboulders described in Eleuthera, Rovere et al. (2017) used geological field surveys to model wave propagation and define boulder transport equations. They concluded that a storm of a “normal amplitude”, meaning of historical intensity, combined with the high sea-level during MIS 5e could have transported the megaboulders from the cliff-edge, thus nuancing the “super storms” and “giant waves” assumption. Following this publication, Hearty and Tormey (2018a) and Rovere et al. (2018) exchanged comments by mutually criticizing each other's methodology.

The impact-generated tsunami explanation, mostly carried by the Holocene Impact Working Group, sparked controversy given its potential significance for past climate reconstructions and future previsions. In fact, the Burckle crater represents one case among hundreds others listed in the Expert Database on Earth Impact Structures (*http://tsun.sscc.ru/nh/impact.php*), defined as “more liberal” than the Earth Impact Database (*http://www.unb.ca/fredericton/science/research/passc/*). Pinter and Ishman (2008), in a concise dissertation and later cited by Bourgeois and Weiss (2009), quoted Carl Sagan (undated), “extraordinary claims require extraordinary evidence” while challenging the mega-tsunami interpretation. They qualified the Burckle crater as “dimple” and stipulated the absence of the associated “impact ejecta” for the K-T impact. According to them, the latter is more likely to be the result of the accumulation of micrometeorites that fall constantly on the surface of the Earth.

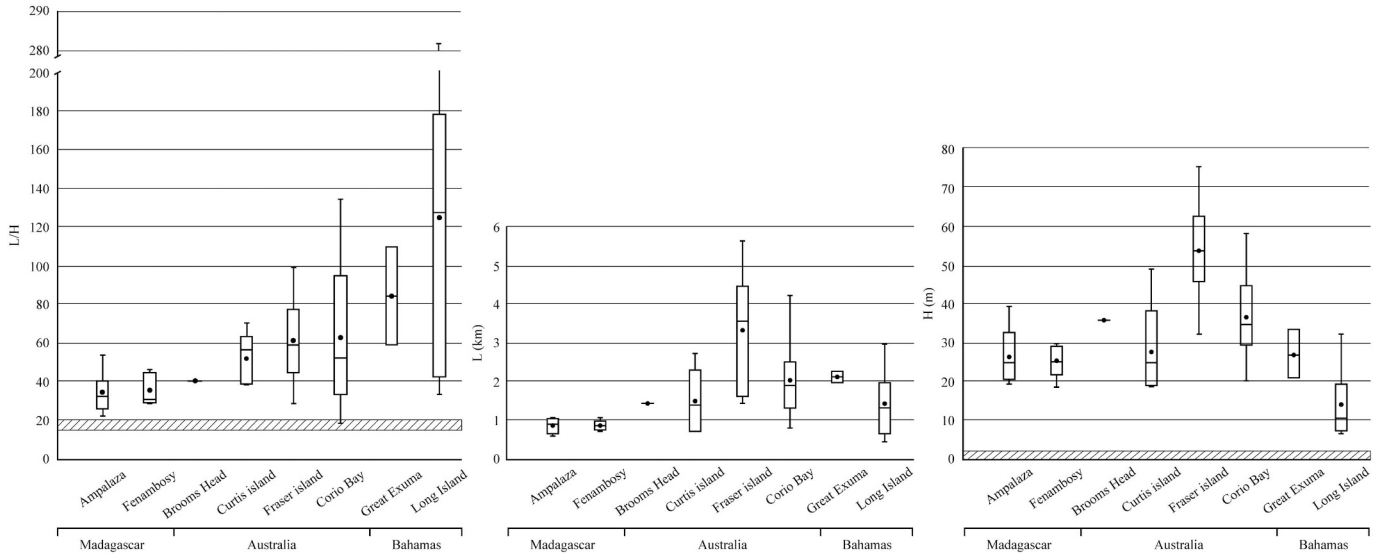

Fig. 8. Distribution of L, H and L/H ratios for each location of the three studied regions where stripped zones indicate the range of subaqueous dunes, after Bourgeois and Weiss (2009), for each parameter. It does not appear on the L graph because of a much smaller order of magnitude.

6. Methods

6.1. GIS analysis

Digital elevation models (DEM) were GIS analyzed to quantify the geomorphological parameters of chevrons in the Bahamas, Madagascar and Queensland. The Fundamental Horizontal Accuracy (FHA) is about 5 m for Queensland, approximatively 12 m for south Madagascar and the Bahamas, whereas the Fundamental Vertical Accuracy (FVA) is respectively of 0.8 m and of 0.0 to 2.0 m (Wessel et al., 2018). Three bedform characteristics were precisely quantified (Fig. 8) to generate a database comparable to that proposed by Bourgeois and Weiss (2009), which was partially based on estimations from the literature: L (km), W (km) and H (m). L is the mean of the lengths of both arms, W is the mean of at least three values measured between the shortest arm and the lobe (defined as where the topography significantly increases beyond the trend of the arm crest), and H is the maximum height measured between the crest and the average altitude of the surrounding floor. For each location, chevrons directions were measured and plotted as rose diagrams (Fig. 9) with their mean ($\bar{x}$), standard deviation (σ) and number of measurements (n).

6.2. Wind analysis

The wind speed-direction data measured by satellite were collected from the POWER Release-8 database of NASA (Stackhouse et al., 2018), and wind parameters were estimated at the 10-m height according to the meteorological convention. They range from January 1st 1990 to January 1st 2017, at the rate of one measurement per day, and were collected for Great Exuma and Long Island in the Bahamas; Ampalaza, Itampolo and Fenambosy in S-Madagascar; and five costal locations (Brooms Head, Corio Bay, Curtis Island, Fraser Island and Moreton Island) in Queensland (Appendix 2). Analyses of wind regimes were performed with WindRose PRO© and plotted as wind roses (Fig. 9). The latter express the distribution of wind speed and direction, using the Beaufort scale where the label “Moderate breeze” corresponds to the impact threshold shear velocity of wind. The amount of data used, the average and maximum speed (in $m.s^{-1}$), and the prevailing wind direction are calculated for each place. To avoid any bias pointed out by several studies (Bullard, 1997; Miot da Silva and Hesp, 2010; Pearce and Walker, 2005; Silva et al., 2008), the collected wind speed data, expressed in $m.s^{-1}$, were converted in knots (kts) when applying the Fryberger method.

6.3. Sand drift potential analysis: The Fryberger method

The Fryberger method (Fryberger and Dean, 1979) uses wind direction and speed to calculate the sand drift potential for the 16 compass points (N, NNE, NE, ENE, E, ESE, SE, SSE, S, SSW, SW, WSW, W, WNW, NW and NNW). Taking up the equation of Lettau (1978), Fryberger and Dean (1979) added the weighting factor for velocity classes (stronger winds have greater weightings) and simplified the equations into:

$$Q \propto V^2(V - V_t)t.$$

where Q is the rate of sand drift expressed in vector units (vu), $V^2(V\text{-}V_t)$ is the weighting factor expressed as a function of the wind velocity V at 10 m height, and the impact threshold shear velocity of wind V_t at 10 m, and t the time wind blew expressed as a percentage. The impact threshold shear velocity (estimated at 12 knots under dry conditions; Fryberger and Dean, 1979) is the minimum velocity of a fluid required to initiate saltation of quartz sand grains (Bagnold, 1936). When carbonate grains are of similar size, shape and density (e.g., ooids), the transport threshold is very similar to that of quartz (Prager et al., 1996).

Once the drift potential values are calculated for all wind speed-direction data, it is possible to retrieve the resultant drift potential (RDP), also expressed in vector units, and the corresponding resultant drift direction (RDD). Because values vary over several order of magnitude, a scale factor (SF) representing a reduction factor was allocated to sand roses for comparison and ease of presentation. A fourth variable, the ratio RDP/DP, was calculated to understand the variability of the wind direction. Ranging from 0 to 1, a high RDP/DP stands for a unidirectional wind regime whereas a low ratio suggests multidirectional winds cancelling each other's DP (Fryberger and Dean, 1979). By combining these variables, the type of wind regime can be categorized (Table 2).

7. Results

Chevrons exhibit lateral extensions ranging from 0.45 to 5.7 km; heights between 7 and 75 m and L/H ratios going from 18 to 282 (Fig. 8). During the past thirty years, winds have blown with an average speed above the impact threshold shear velocity (~5.5 $m.s^{-1}$) in most studied places, except at Brooms Head and Moreton Island (Fig. 9). In

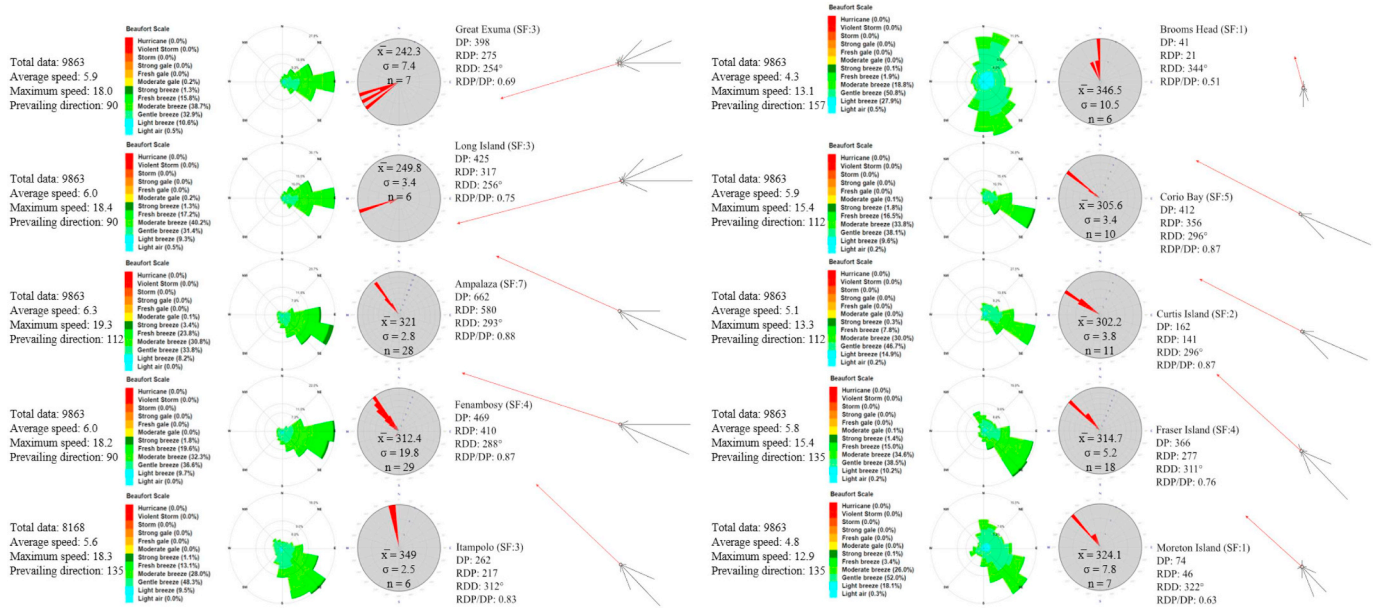

Fig. 9. Columns 1–3 and 6–8: Wind regimes analyses with average and maximum speed plus the prevailing direction of wind. Proportions of each Beaufort class expressed in percentages of the time wind blew, next to windroses. Column 4 and 9: Rose diagrams showing the measured orientations of chevron ridges with the average direction, standard deviation and number of measurements. Column 5 and 10: Sand roses obtained by DP analysis with total DP, RDP, RDD and RDP/DP. (For interpretation of the references to colour in this figure legend, the reader is referred to the web version of this article.)

Great Exuma and Long Island, wind conditions with the capacity to trigger saltation represent respectively 56% and 59% of the time. In South Madagascar, it is 58% in Ampalaza, 54% in Fenambosy and 42% in Itampolo. Finally, wind blows above the threshold 21%, 52%, 38%, 51% and 30% of the time respectively in Brooms Head, Corio Bay, Curtis Island, Fraser Island and Moreton Island.

Chevrons (aka parabolic dunes according to many authors in many of the mentioned locations) azimuths show a narrow distributivity with a maximum standard deviation of 19.8 for the Fenambosy site, and a strong correlation with RDD (Fig. 10). DPs indicate a wide variety of environments in terms of wind energy, but every time under a system that tends to be unimodal with RDP/DP ratios within obtuse/acute bimodal to wide/narrow unimodal ranges (Table 2).

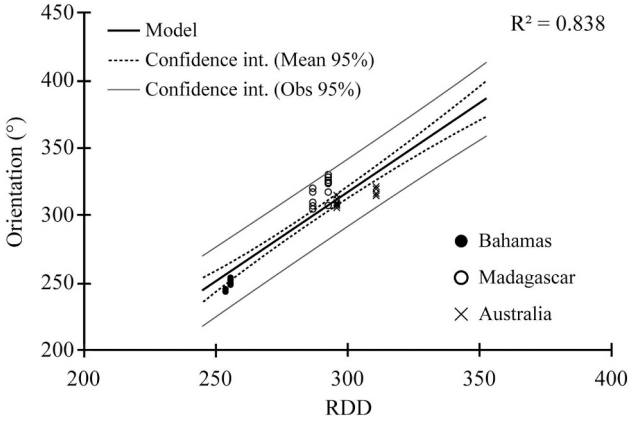

Fig. 10. Linear regression model for chevrons azimuths on RDD showing a strong correlation between the two variables.

8. Discussion

The morphological parameters of chevrons need to be interpreted by region for obvious reasons such as difference in composition, ground, vegetation, precipitation rate, climatic zone and sediment supply. Since the most extended and highest dunes are not necessarily the ones associated with the greatest DP, RDP or the most unimodal wind regimes, L and H should be controlled by other factors (Hack, 1941; Hugenholtz, 2010; Rubin and Hunter, 1982; Wasson and Hyde, 1983). However, distribution of L, H and L/H of chevrons is undoubtedly above the range of subaqueous bedforms and correspond to values given for parabolic dunes (Bourgeois and Weiss, 2009; Lancaster, 1994).

The wind regimes and drift potential analyses reveal that wind blows above the impact threshold shear velocity with an acute bimodal or unimodal configuration most of the time, and for the great majority

Table 2
Fryberger's classification of wind regimes (Fryberger and Dean, 1979) using DP analysis and the corresponding studied locations (this study).

DP (vu)	DP (m3 m-1 year-1)	Energy of wind direction	Locations
< 200	< 17	Low	Brooms Head, Moreton island, Curtis island
200–400	17–33	Intermediate	Itampolo, Fraser island, Great Exuma
> 400	> 33	High	Corio Bay, Long Island, Fenambosy, Ampalaza

RDP/DP	Variability	Probable category	Locations
< 0.3	Low	Complex / Obtuse bimodal	
0.3–0.8	Intermediate	Obtuse / Acute bimodal	Brooms Head, Moreton island, Great Exuma, Long Island, Fraser island
> 0.8	High	Wide / Narrow unimodal	Itampolo, Curtis island, Corio Bay, Fenambosy, Ampalaza

of the studied locations. Despite wind regimes being low, intermediate and high energy environment, the dominant Beaufort class to blow and actively induce grain mobilization in every region is the "moderate breeze" (5.5 to 7.9 $m.s^{-1}$). In this environment, chevrons azimuths are strongly correlated to RDD (Fig. 10), which suggests an eolian origin for these deposits. The studied chevrons lie in different regions corresponding to different climate zones, vegetation type, sediment availability and composition. The Bahamas and South-Madagascar are classified as tropical savanna climates (*Aw*) according to the Köppen climate classification (Peel et al., 2007), which have a pronounced dry season (< 60 mm of precipitations for the driest month) and a wet season that receives less precipitation than the similar tropical monsoon season. Usually, this category is characterized by tall grass and short deciduous trees or rampant-type vegetation. The studied areas in Queensland lie in a humid subtropical climate zone (*Cfa*), defined by hot and humid summers, and mild to chilly winters. The vegetation comprises evergreen trees, shrubs and bushes. The annual precipitation ranges from 1000 to 2000 mm, moistening sand and increasing the impact threshold minimum. The different types of vegetation, which plays a key role in stabilizing the arms of the dune and driving the parabolic shape, act differently on sand migration in the considered regions. Nonetheless, the recurrence of the "U" and "V" shape, the correlation between chevrons azimuths and RDD, and the similar type of wind regimes agrees with Wolman and Miller (1960) and Bagnold (1941), who showed that net transport, dune form and orientation are parameters controlled by recurring winds above the impact threshold rather than by brief sporadic episodes of wind gusts.

As it has been a major argument to seek for alternative explanations concerning their formation, the Fryberger method proves that chevrons are effectively aligned with the dominant ***drift potential*** direction, which agrees with the principle of Occam's Razor cited by Bourgeois and Weiss (2009): the simpler explanation is usually the better. Regarding the numerous arguments given in the literature and the new data provided in this study, it is reasonable to argue that chevrons are mostly, if not all parabolic dunes and that scientists should get rid of the term "chevron", which has proven to be confusing, and provides little to no indication of the true genesis of most deposits claimed to be such.

So not only does wind regime control the orientation of landforms, but it is also a major component of processes shaping parabolic dune complexes or dune-field systems. One of the most interesting aspect of the data is the correlation between present wind regimes and some morphological parameters of Holocene or Pleistocene-dated chevrons. Thus, the latter seem to act as paleo-wind proxies arguing for unchanged wind regimes, at least of drift potential directions, since the LIG. Wind regimes during Holocene are more easily studied because it is a recent period, but as stated by Opdyke (1961), the wind belts during the Pleistocene were similar to the present ones, despite a significant difference in global temperature (Mackenzie, 1964). Given the wide distribution of "chevrons" on the world's coasts (Fig. 1), they could be useful to reconstruct global paleo-wind circulation at different periods of the recent past.

9. Conclusions

We have reviewed the distribution, morphology, sedimentological characteristics, geochronology, and the different interpretations pertaining to the mode of formation of chevron ridges. We further proposed a general wind-related analysis in three coastal locations along three oceans in two different climate zones. The main conclusions of this review and of our new analysis are as follows:

- Chevron ridges are commonly found lying on or near coastlines but can also be observed in continental interiors.
- There are eight different types of so-called chevron, actually parabolic dune, morphologies, six of which exhibit a central depression framed by elevated crests. Alleged chevrons have a km-scale length, tens to thousands m-size width and a plurimetric thickness. The measured values for these morphological parameters are well above the range of subaqueous bedforms and correspond to values given for parabolic dunes
- Sedimentological features commonly present within chevrons are subparallel, low-angle, aggrading, seaward dipping beds with few interruptions and truncations. An alternation with cm-scale, fenestrae-rich beds can be observed in the Bahamas occurrences. Some authors have also observed subcritically climbing translatent strata (SCTS) which are typical of eolian transport.
- The age of the studied chevrons extends from the LIG and the Late Holocene.
- Chevrons azimuths show a narrow distributivity and a strong correlation with the resultant drift direction (RDD) of the wind, whereas in many cases, they are not aligned with the dominant swell or estimated wave directions associated with possible tsunamis, or similar.

The presence of characteristic eolian sedimentary features (SCTS) within chevrons and the correlation of their morphology with wind regimes rather suggest that strong unidirectional, constantly-blowing winds reworking exposed subtidal to intertidal and backshore sediments are a more plausible explanation for their origin than a rapid dramatic hydrodynamic process. Consequently, the term "chevron" should be banned from the literature if it is to be used as defined in this paper, in order to avoid any possible confusion. Finally, these deposits appear to be a useful tool to reconstruct wind environments of the past and constrain paleoclimatic models.

Acknowledgments

This project was funded by the department of Geology of the University of Geneva. Many thanks to the Earth Observation Center at the German Aerospace Center (DLR) for generously providing the DEMs needed. We acknowledge André Strasser for his guidance during the initial stages of writing this review. We thank Patrick Hesp for his detailed and helpful review that provided us the guidance to improve this manuscript.

Appendix A. Appendices

Appendix 1

: Compilation of all dating data available in literature for chevrons. (1) sample taken at −0.6 m; (2) sample taken at -2 m; (3) sample taken at -10 m; (4) sample taken at -20 m; (5) sample taken at -25 m; (6) sample taken at -8 m, minimum age; (7) sample taken at −6 to -8 m; (8) sample taken just below (7); (9) reliable age; (10) minimum age; (11) maximum age; (12) High U and Th content; (13) High U and Th content

Country	Region	Location	Stratigraphy	Method	Age	Reference
Bahamas	Long Island	Miller's Settlement	French Bay Member	WR A/I	Late Pleistocene, MIS 5e	Hearty et al., 1998
Egypt	S-Egypt	Selima sand sheet	Actual	Sattelite images and field study	Actual	Maxwell and Haynes, 1989

(*continued on next page*)

Appendix 1 (*continued*)

Country	Region	Location	Stratigraphy	Method	Age	Reference
Madagascar	S-Madagascar	Ampalaza Bay		Geomorphic indicators and archeologic dating	Mid Holocene to 500 CE	Gusiakov et al., 2009
		Fenambosy		Geomorphic indicators and archeologic dating	Mid Holocene to 500 CE	Gusiakov et al., 2009
		Cap *St.* Marie		Geomorphic indicators and archeologic dating	Mid Holocene to 500 CE	Gusiakov et al., 2009
		Faux Cap		Geomorphic indicators and archeologic dating	Mid Holocene to 500 CE	Gusiakov et al., 2009
		Ambazoa		Geomorphic indicators	3000–2000 BP or 18,000 BP	Clark et al., 1998
W-Australia		Quobba		Geomorphic indicators	Younger Pleistocene	Scheffers et al., 2008
		South Coral Bay		Geomorphic indicators	Pleistocene	Scheffers et al., 2008
		West Albany		Geomorphic indicators	Pleistocene	Scheffers et al., 2008
N-Australia		Groote Eylandt		Geomorphic indicators	Holocene	Scheffers et al., 2008
E-Australia	Cape Bedord-Cape Flattery dunefield	NW of Cape Flattery	First unit (oldest)	^{14}C	> 48′000	Pye and Switsur, 1981
		Near Cape Flattery Mining Camp	Second unit	^{14}C	7′480 ± 75 BP	Pye and Switsur, 1981
				^{14}C	7′560 ± 90 BP	Pye and Switsur, 1981
				^{14}C	8′200 ± 85 BP	Pye and Switsur, 1981
			Third unit (youngest); A for Lee et al., 1990	Aerial photographs	300–500	Pye, 1993
		Near Red Hill	A	^{14}C	220 ± 70 BP (1)	Lees et al., 1990
			B	Thermoluminescence	2′000 ± 1000 BP (2)	Lees et al., 1990
			C	Thermoluminescence	19′200 ± 3400 BP (3)	Lees et al., 1990
			D	Thermoluminescence	22′700 ± 2800 BP (4)	Lees et al., 1990
			E	Thermoluminescence	19′800 ± 2300 BP (5)	Lees et al., 1990
			F	Thermoluminescence	171′000 ± 13,000 BP	Lees et al., 1990
			G	Thermoluminescence	> 66′000 BP	Lees et al., 1990
	Shelburne Bay dunefield	Red Cliffs	C	Thermoluminescence	17′600 ± 1400 BP (6)	Lees et al., 1990
			D	Thermoluminescence	28′400 ± 1300 BP (7)	Lees et al., 1990
			D	Thermoluminescence	29′900 ± 2400 BP (8)	Lees et al., 1990
			D	^{14}C	29′740 ± 3030 BP (9)	Lees et al., 1990
		Double Point	C	Thermoluminescence	23′800 ± 2400 BP	Lees et al., 1990
		Conical Hill	C	Thermoluminescence	15′000 ± 1110 BP (10)	Lees et al., 1990
		?	A	^{14}C	930 ± 135 BP (11)	Lees et al., 1990
	Arnhem Land dunefields	Cobourg Peninsula	B	Thermoluminescence	1′900 ± 400 BP	Lees et al., 1990
			C	Thermoluminescence	2′600 ± 300 BP	Lees et al., 1990
			C	Thermoluminescence	2′800 ± 500 BP	Lees et al., 1990
				Thermoluminescence	8′600 ± 1400 BP	Lees et al., 1990
			E	Thermoluminescence	9′300 ± 1100 BP (12)	Lees et al., 1990
			E	Thermoluminescence	81′400 ± 8500 BP (13)	Lees et al., 1990
	Hinchinbrook Island	Ramsay Bay		^{14}C	9′000 BP	Pye, 1993
				^{14}C	900 BP	Pye, 1993

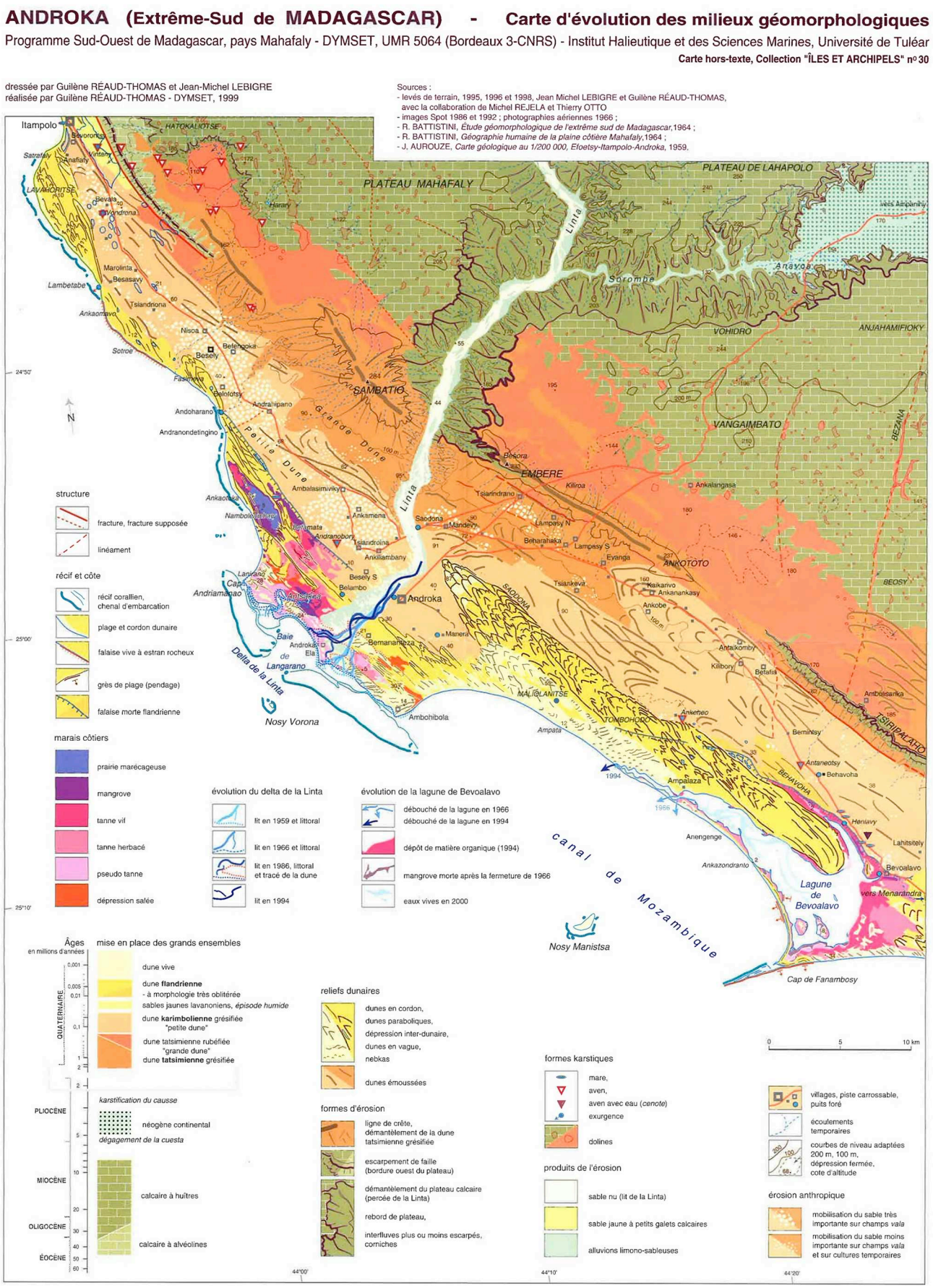

Appendix 2. : Geomorpholy and stratigraphy of the extreme S-Madagascar (from Lebigre et al., 2001)

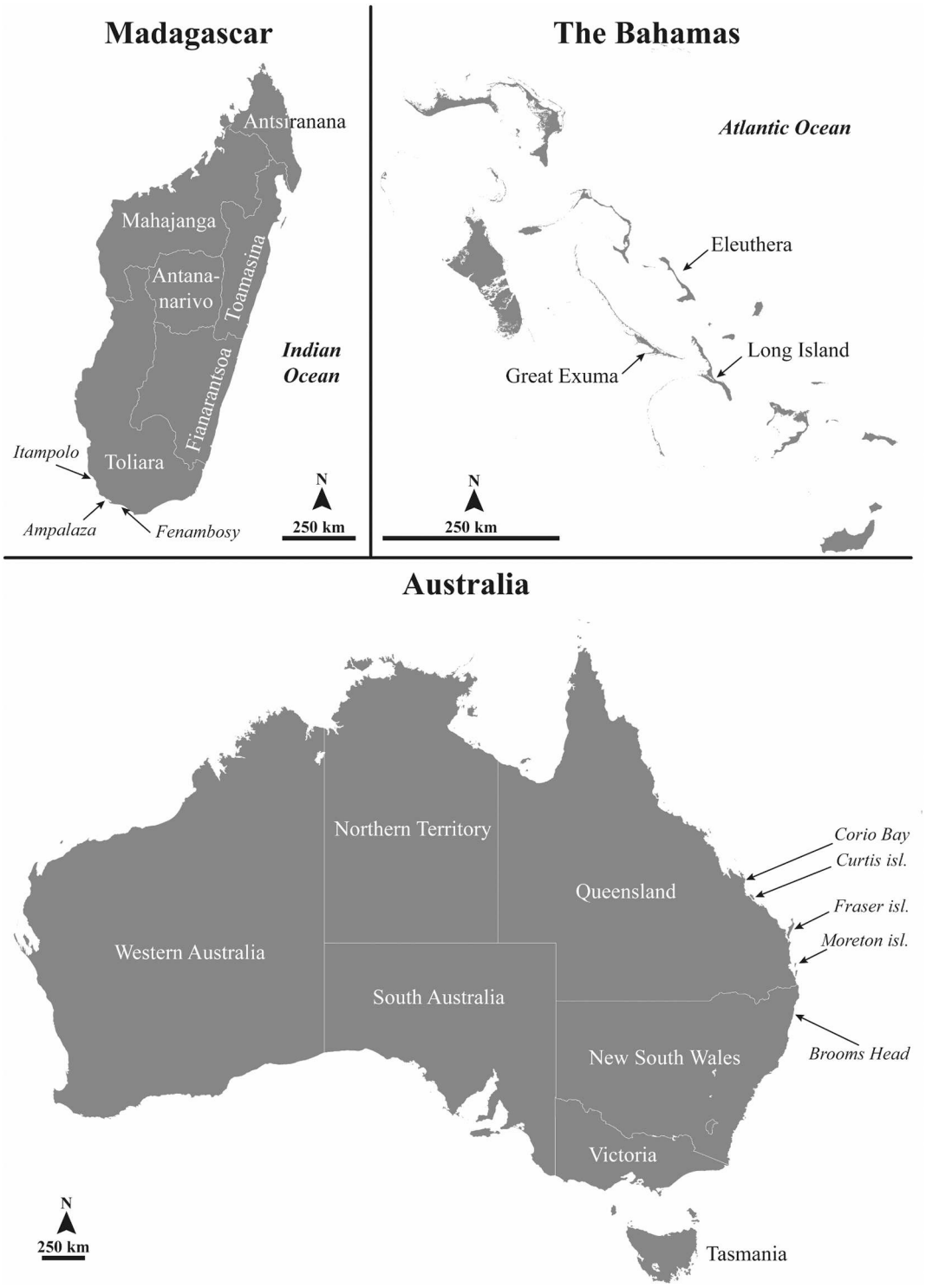

Appendix 3. : Map of Madagascar, the Bahamas and Australia showing the studied locations

References

Abbott, D., 2006. Impact Craters as sources of Megatsunami Generated Chevron Dunes. In: Presented at the GSA Philadelphia Annual Meeting, Philadelphia.

Abbott, D.H., Masse, W.B., Burckle, L.D., Breger, D.L., Gerard-Little, P., 2005. Burckle abyssal impact crater: Did this impact produce a global deluge?.

Abbott, D., Bryant, E., Gusiakov, V., Masse, W., Raveloson, A., Razafindrakoto, H., 2006. Report of International Tsunami Expedition to Madagascar.

Abbott, D., Bryant, T., Gusiakov, V., Masse, W., 2007. Megatsunami of the World Ocean: Did they Occur in the Recent Past? presented at the AGU Spring Meeting.

Allen, R.J.L., 1982. Sedimentary structures, their character and physical basis (Vol. 1). Elsevier, Amsterdam.

Bagnold, R., 1936. The movement of desert sand. Proc. R. Soc. Lond. Ser. Math. Phys. Sci. 157, 594–620.

Bagnold, R., 1941. The Physics of Blown Sand and Desert Dunes. William Morrow & Company, New York, NY.

Bain, R., Kindler, P., 1994. Irregular fenestrae in Bahamian eolianites: a rainstorm-induced origin. J. Sediment. Res. 64.

Battistini, R., 1964. L'Extrême-Sud de Madagascar, étude géomorphologique. (Paris).

Blench, R., 2010. Evidence for the Austronesian voyages in the Indian Ocean. The global origins and development of seafaring. 239. pp. 48.

Bourgeois, J., Weiss, R., 2009. "Chevrons" are not mega-tsunami deposits - a sedimentologic assessment. Geology 37, 403–406. https://doi.org/10.1130/G25246A.1.

Bowen, A., Lindley, D., 1977. A wind-tunnel investigation of the wind speed and turbulence characteristics close to the ground over various escarpment shapes. Bound.-Layer Meteorol. 12, 259–271. https://doi.org/10.1007/BF00121466.
Bryant, E., 2014. Tsunami: The Underrated Hazard. Springer.
Bryant, E., Nott, J., 2001. Geological indicators of large tsunami in Australia. Nat. Hazards 24, 231–249.
Bryant, E., Young, R., Price, D., Wheeler, D., Pease, M., 1997. The impact of tsunami on the coastline of Jervis Bay, southeastern Australia. Phys. Geogr. 18, 440–459.
Bryant, E., Walsh, G., Abbott, D., 2007. Cosmogenic mega-tsunami in the Australia region: are they supported by Aboriginal and Maori legends? Geol. Soc. Lond. Spec. Publ. 273, 203–214.
Bullard, J., 1997. A note on the use of the "Fryberger method" for evaluating potential sand transport by wind. J. Sediment. Res. 67, 499–501. https://doi.org/10.1306/D42685A9-2B26-11D7-8648000102C1865D.
Clark, C.D., Garrod, S.M., Pearson, M.P., 1998. Landscape archaeology and remote sensing in southern Madagascar. International Journal of Remote Sensing 19 (8), 1461–1477.
DeConto, R., Pollard, D., 2016. Contribution of Antarctica to past and future sea-level rise. Nature 531, 591–597. https://doi.org/10.1038/nature17145.
Burney, D.A., Burney, L.P., Godfrey, L.R., Jungers, W.L., Goodman, S.M., Wright, H.T., Jull, A.T., 2004. A chronology for late prehistoric Madagascar. Journal of Human Evolution 47 (1-2), 25–63.
Donnelly, C., Kraus, N., Larson, M., 2006. State of knowledge on measurement and modeling of coastal overwash. Journal of coastal research 965–991.
Engel, M., Kindler, P., Godefroid, F., 2015. Interactive comment on "Ice melt, sea level rise and superstorms: evidence from paleoclimate data, climate modeling, and modern observations that 2° C global warming is highly dangerous" by J. Hansen et al. Atmos. Chem. Phys. Discuss. 15, C6270–C6281.
Fryberger, S.G., Dean, G., 1979. Dune forms and wind regime. In A study of global sand seas 1052, 137–169 US Government Printing Office Washington.
Fryberger, S., Schenk, C., 1988. Pin stripe lamination: a distinctive feature of modern and ancient eolian sediments. Sediment. Geol. 55, 1–15.
Gusiakov, V., Abbott, D., Bryant, E.A., Masse, W., Breger, D., 2009. Mega Tsunami of the World Oceans: Chevron Dune Formation, Micro-Ejecta, and Rapid climate Change as the evidence of recent Oceanic Bolide Impacts. In: Beer, T. (Ed.), Geophysical Hazards. Springer Netherlands, Dordrecht, pp. 197–227. https://doi.org/10.1007/978-90-481-3236-2_13.
Hack, J., 1941. Dunes of the Western Navajo Country. Geogr. Rev. 31, 240. https://doi.org/10.2307/210206.
Hansen, J., Kharecha, P., Sato, M., Masson-Delmotte, V., Ackerman, F., Beerling, D., Hearty, P., Hoegh-Guldberg, O., Hsu, S.-L., Parmesan, C., Rockstrom, J., Rohling, E., Sachs, J., Smith, P., Steffen, K., Van Susteren, L., von Schuckmann, K., Zachos, J., 2013. Assessing "dangerous climate Change": required Reduction of Carbon Emissions to Protect Young People, Future Generations and Nature. PLoS ONE 8, e81648. https://doi.org/10.1371/journal.pone.0081648.
Hansen, J., Sato, M., Hearty, P., Ruedy, R., Kelley, M., Masson-Delmotte, V., Russell, G., Tselioudis, G., Cao, J., Rignot, E., Velicogna, I., Kandiano, E., von Schuckmann, K., Kharecha, P., Legrande, A., Bauer, M., Lo, K.-W., 2015. Ice melt, sea level rise and superstorms: evidence from paleoclimate data, climate modeling, and modern observations that 2 °C global warming is highly dangerous. Atmos. Chem. Phys. Discuss. 15, 20059–20179. https://doi.org/10.5194/acpd-15-20059-2015.
Hays, J., Imbrie, J., Shackleton, N., 1976. Variations in the Earth's Orbit: pacemaker of the Ice Ages. Science 194, 13.
Hearty, P., 1997. Boulder Deposits from large Waves during the last Interglaciation on North Eleuthera Island, Bahamas. Quat. Res. 48, 326–338. https://doi.org/10.1006/qres.1997.1926.
Hearty, P., Kaufman, D., 2000. Whole-Rock Aminostratigraphy and Quaternary Sea-Level history of the Bahamas. Quat. Res. 54, 163–173. https://doi.org/10.1006/qres.2000.2164.
Hearty, P., Kaufman, D., 2009. A Cerion-based chronostratigraphy and age model from the central Bahama Islands: Amino acid racemization and 14C in land snails and sediments. Quat. Geochronol. 4, 148–159. https://doi.org/10.1016/j.quageo.2008.08.002.
Hearty, P., Tormey, B., 2017. Sea-level change and superstorms; geologic evidence from the last interglacial (MIS 5e) in the Bahamas and Bermuda offers ominous prospects for a warming Earth. Mar. Geol. 390, 347–365. https://doi.org/10.1016/j.margeo.2017.05.009.
Hearty, P., Tormey, B., 2018a. Discussion of: Mylroie, JE, 2018. Superstorms: comments on Bahamian Fenestrae and Boulder evidence from the last Interglacial. J. Coast. Res. 34 (6), 1471–1483. (1503–1511). https://doi.org/10.2112/JCOASTRES-D-18A-00003.1.
Hearty, P., Tormey, B., 2018b. Listen to the whisper of the rocks, telling their ancient story. Proc. Natl. Acad. Sci. 115, E2902–E2903. https://doi.org/10.1073/pnas.1721253115.
Hearty, P., Neumann, A., Kaufman, D., 1998. Chevron ridges and runup deposits in the Bahamas from storms late in oxygen-isotope substage 5e. Quat. Res. 50, 309–322.
Hearty, P., Tormey, B., Neumann, A., 2002. Discussion of "Palaeoclimatic significance of co-occurring wind-and water-induced sedimentary structures in the last-interglacial coastal deposits from Bermuda and the Bahamas"(Kindler and Strasser, 2000, Sedimentary Geology, 131, 1–7). Sediment. Geol. 147, 429–435.
Hearty, P., Hollin, J., Neumann, A., O'Leary, M., McCulloch, M., 2007. Global sea-level fluctuations during the last Interglaciation (MIS 5e). Quat. Sci. Rev. 26, 2090–2112. https://doi.org/10.1016/j.quascirev.2007.06.019.
Hesp, P., 2011. Dune Coasts. In: Treatise on Estuarine and Coastal Science. Elsevier, pp. 193–221. https://doi.org/10.1016/B978-0-12-374711-2.00310-7.
Hesp, P., Chape, S., 1984. 1:3 Million Map of the Coastal Environment of Western Australia.
Hesp, P., Walker, I., 2013. Coastal dunes. In: Treatise on Geomorphology.
Hollin, J., 1965. Wilson's theory of ice ages. Nature 208, 12–16. https://doi.org/10.1038/208012a0.
Hugenholtz, C., 2010. Topographic changes of a supply-limited inland parabolic sand dune during the incipient phase of stabilization. Earth Surf. Process. Landf. 35, 1674–1681. https://doi.org/10.1002/esp.2053.
Hunter, R., 1977. Basic types of stratification in small eolian dunes. Sedimentology 24, 361–387.
Jackson, P., 1975. A theory for flow over escarpments. In: Presented at the Fourth International Conf. On Wind Effects on Buildings and Structures. Heathrow, UK, pp. 40.
Jennings, J., 1957. On the Orientation of Parabolic or U-Dunes. Geogr. J. 123, 474. https://doi.org/10.2307/1790349.
Jennings, J., 1967. Cliff-top dunes. Aust. Geogr. Stud. 5, 40–49.
Kelletat, D., Scheffers, A., 2003. Chevron-shaped accumulations along the coastlines of Australia as potential tsunami evidences. Sci. Tsunami Hazards 21, 174–188.
Kindler, P., 1991. Keystone vugs in coastal dunes: an example from the Pleistocene of Eleuthera, Bahamas. In: Presented at the Proceedings of the Fifth Symposium on the Geology of the Bahamas. Bahamian Field Station, San Salvador, Bahamas, pp. 117–123.
Kindler, P., Hearty, P., 1996. Carbonate petrography as an indicator of climate and sea-level changes: new data from Bahamian Quaternary units. Sedimentology 43, 381–399. https://doi.org/10.1046/j.1365-3091.1996.d01-11.x.
Kindler, P., Strasser, A., 2000. Palaeoclimatic significance of co-occurring wind-and water-induced sedimentary structures in the last-interglacial coastal deposits from Bermuda and the Bahamas. Sediment. Geol. 131, 1–7.
Kindler, P., Strasser, A., 2002. Palaeoclimatic significance of co-occurring wind- and water-induced sedimentary structures in last-interglacial coastal deposits from Bermuda and the Bahamas: response to Hearty et al.'s comment. Sediment. Geol. 147, 437–443. https://doi.org/10.1016/S0037-0738(01)00099-9.
Kopp, R., Simons, F., Mitrovica, J., Maloof, A., Oppenheimer, M., 2009. Probabilistic assessment of sea level during the last interglacial stage. Nature 462, 863–867. https://doi.org/10.1038/nature08686.
Lancaster, N., 1994. Dune morphology and dynamics. In: Geomorphology of Desert Environments, pp. 474–505 Dordrecht.
Lebigre, J.-M., Réaud-Thomas, G., Rejela, M., 2001. In: Cret (Ed.), Androka (Extrême-Sud de Madagascar): cartes d'évolution des milieux. Iles et Archipels, Bordeaux.
Lees, B., Yanchou, L., Head, J., 1990. Reconnaissance Thermoluminescence Dating of Northern Australian Coastal Dune Systems. Quat. Res. 34, 169–185. https://doi.org/10.1016/0033-5894(90)90029-K.
Lettau, K., 1978. Experimental and micrometeorological field studies of dune migration. In: Exploring in the World's Driest Climate, pp. 110–147.
Mackenzie, F., 1964. Bermuda pleistocene eolianites and paleowinds1. Sedimentology 3, 52–64. https://doi.org/10.1111/j.1365-3091.1964.tb00275.x.
Marsh, W., Marsh, B., 1987. Wind Erosion and Sand Dune Formation on High Lake Superior Bluffs. Geogr. Ann. Ser. Phys. Geogr. 69, 379–391.
Masse, W., 2007. The archaeology and anthropology of Quaternary period cosmic impact. In: Comet/Asteroid Impacts and Human Society. An Interdisciplinary Approach. Berlin Heidelberg, pp. 25–70.
Masse, W., Masse, M., 2007. Myth and catastrophic reality: using myth to identify cosmic impacts and massive Plinian eruptions in Holocene South America. Geol. Soc. Lond. Spec. Publ. 273, 177–202.
Masse, W., Bryant, E., Gusiakov, V., Abbott, D., Rambolamana, G., Raza, H., Courty, M., Breger, D., Gerard-Little, P., Burckle, L., 2006. Holocene Indian Ocean cosmic impacts: the megatsunami chevron evidence from Madagascar. In: AGU Fall Meeting Abstracts.
Masson-Delmotte, V., Schulz, M., Abe-Ouchi, A., Beer, J., Ganopolski, A., González Rouco, J., Jansen, E., Lambeck, K., Luterbacher, J., Naish, T., et al., 2013. Information from paleoclimate archives. Clim. Chang. 383–464 The Physical Science Basis.
Maxwell, T., Haynes, C., 2001. Sand sheet dynamics and Quaternary landscape evolution of the Selima Sand Sheet, southern Egypt. Quaternary Science Reviews 20 (15), 1623–1647.
McKee, E., 1979. A study of global sand seas. Geol. Surv. Prof. Pap. 439.
Mercer, J., 1978. West Antarctic ice sheet and CO2 greenhouse effect: a threat of disaster. Nature 271, 321.
Miot da Silva, G., Hesp, P., 2010. Coastline orientation, aeolian sediment transport and foredune and dunefield dynamics of Moçambique Beach, Southern Brazil. Geomorphology 120, 258–278. https://doi.org/10.1016/j.geomorph.2010.03.039.
Mylroie, J., 2018a. Superstorms: comments on Bahamian fenestrae and boulder evidence from the last interglacial. J. Coast. Res. 34, 1471–1483. https://doi.org/10.2112/JCOASTRES-D-17-00215.1.
Mylroie, J., 2018b. Reply to: Hearty, P.J. and Tormey, B.R., 2018. Discussion of: Mylroie, J.E., 2018. Superstorms: comments on Bahamian Fenestrae and Boulder evidence from the last Interglacial. *Journal of Coastal Research,* 34(6), 1471–1483. J. Coast. Res. 346, 1512–1515. https://doi.org/10.2112/JCOASTRES-D-18A-00004.
Neumann, A., Hearty, P., 1996. Rapid sea-level changes at the close of the last interglacial (substage 5e) recorded in Bahamian island geology. Geology 24, 775–778.
O'Leary, M., Hearty, P., Thompson, W., Raymo, M., Mitrovica, J., Webster, J., 2013. Ice sheet collapse following a prolonged period of stable sea level during the last interglacial. Nat. Geosci. 6, 796–800. https://doi.org/10.1038/ngeo1890.
Opdyke, N., 1961. The palaeoclimatological significance of desert sandstone. In: Descriptive Palaeoclimatology, pp. 45–60 New York, NY.
Pearce, K., Walker, I., 2005. Frequency and magnitude biases in the 'Fryberger' model, with implications for characterizing geomorphically effective winds. Geomorphology 68, 39–55. https://doi.org/10.1016/j.geomorph.2004.09.030.

Peel, M., Finlayson, B., McMahon, T., 2007. Updated world map of the Köppen-Geiger climate classification. Hydrol. Earth Syst. Sci. Discuss. 4, 439–473.
Pinter, N., Ishman, S., 2008. Impacts, mega-tsunami, and other extraordinary claims. GSA Today 18, 37. https://doi.org/10.1130/GSAT01801GW.1.
Prager, E., Southard, J., Vivoni-Gallart, E., 1996. Experiments on the entrainment threshold of well-sorted and poorly sorted carbonate sands. Sedimentology 43, 33–40. https://doi.org/10.1111/j.1365-3091.1996.tb01457.x.
Pye, K., 1982a. Negatively skewed aeolian sands from a humid tropical coastal Dunefield, Northern Australia. Sediment. Geol. 31, 249–266. https://doi.org/10.1016/0037-0738(82)90060-4.
Pye, K., 1982b. Morphological Development of Coastal Dunes in a Humid Tropical Environment, Cape Bedford and Cape Flattery, North Queensland. Geogr. Ann. Phys. Geogr. 64, 16.
Pye, K., 1983. Dune formation on the humid tropical sector of the North Queensland Coast, Australia. Earth Surf. Process. Landf. 8, 371–381. https://doi.org/10.1002/esp.3290080409.
Pye, K., Lancaster, N., 1993. Late quaternary development of coastal parabolic megadune complexes in Northeastern Australia. In: Pye, K. (Ed.), Aeolian Sediments. Blackwell Publishing Ltd, Oxford, UK, pp. 23–44. https://doi.org/10.1002/9781444303971.ch3.
Pye, K., Mazzullo, S., 1994. Effects of Tropical Weathering on Quartz Grain Shape: an example from Northeastern Australia. SEPM J. Sediment. Res. 64A. https://doi.org/10.1306/D4267DE8-2B26-11D7-8648000102C1865D.
Pye, K., Rhodes, E., 1985. Holocene development of an episodic transgressive dune barrier, Ramsay Bay, North Queensland, Australia. Mar. Geol. 64, 189–202. https://doi.org/10.1016/0025-3227(85)90104-5.
Pye, K., Switsur, V., 1981. Radiocarbon dates from the Cape Bedford and Cape Flattery dunefields, North Queensland. Search 12, 225–226.
Pye, K., Tsoar, H., 2008. Aeolian Sand and Sand Dunes. Springer Science & Business Media.
Ramsay, J.G., 1974. Development of chevron folds. Geological Society of America Bulletin 85 (11), 1741–1754.
Rovere, A., Casella, E., Harris, D., Lorscheid, T., Nandasena, N., Dyer, B., Sandstrom, M., Stocchi, P., D'Andrea, W., Raymo, M., 2017. Giant boulders and last Interglacial storm intensity in the North Atlantic. Proc. Natl. Acad. Sci. 114, 12144–12149. https://doi.org/10.1073/pnas.1712433114.
Rovere, A., Casella, E., Harris, D., Lorscheid, T., Nandasena, N., Dyer, B., Sandstrom, M., Stocchi, P., D'Andrea, W., Raymo, M., 2018. Reply to Hearty and Tormey: use the scientific method to test geologic hypotheses, because rocks do not whisper. Proc. Natl. Acad. Sci. 115, E2904–E2905. https://doi.org/10.1073/pnas.1800534115.
Rubin, D., Hunter, R., 1982. Bedform climbing in theory and nature. Sedimentology 29, 121–138.
Scheffers, A., Kelletat, D., 2003. Sedimentologic and geomorphologic tsunami imprints worldwide—a review. Earth-Sci. Rev. 63, 83–92. https://doi.org/10.1016/S0012-8252(03)00018-7.
Scheffers, A., Kelletat, D., Scheffers, S., Abbott, D., Bryant, E., 2008. Chevrons – enigmatic sedimentary coastal features. Z. Für Geomorphol. 52, 375–402. https://doi.org/10.1127/0372-8854/2008/0052-0375.
Schwartz, R., 1982. Bedform and stratification characteristics of some modern small-scale washover sand bodies. Sedimentology 29, 835–849.
Shen, H., Julien, P., 1993. Erosion and sediment transport. In: Handbook of Hydrology, (New York, NY).
Short, A., 1988. Holocene coastal dune formation in southern Australia: a case study. Sediment. Geol. 55, 121–142.
Short, A., 2005. Beaches of the Western Australian Coast: Eucla to Roebuck Bay: A Guide to their Nature, Characteristics, Surf and Safety. Sydney University Press. ed.
Short, A., 2006. Australian Beach Systems—Nature and distribution. J. Coast. Res. 221, 11–27. https://doi.org/10.2112/05A-0002.1.
Short, A., 2014. The Australian Coast: Teacher Notes and Student Activities. Geoscience Australia.
Shulmeister, J., Lees, B., 1992. Morphology and chronostratigraphy of a coastal dunefield; Groote Eylandt, northern Australia. Geomorphology 5, 521–534. https://doi.org/10.1016/0169-555X(92)90023-H.
Silva, G., Hesp, P., Peixoto, J., Dillenburg, S., 2008. Foredune vegetation patterns and alongshore environmental gradients: Moçambique Beach, Santa Catarina Island, Brazil. Earth Surf. Process. Landf. 33, 1557–1573. https://doi.org/10.1002/esp.1633.
Stackhouse, P., Zhang, T., Westberg, D., Barnett, A., Bristow, T., Macpherson, B., Hoell, J., 2018. POWER Release 8 (with GIS Applications) Methodology (Data Parameters, Sources, and Validation—Data Version 8.0. 1). NASA Langley Research Center, Hampton, VA, USA.
Stieglitz, R., Inden, R., 1969. Development of cavernous sediment in a non-beach environment. J. Sediment. Res. 39, 342–344.
Tejan-Kella, M., Chittleborough, D., Fitzpatrick, R., Thompson, C., Prescott, J., Hutton, J., 1990. Thermoluminescence dating of coastal sand dunes at Cooloola and North Stradbroke Island, Australia. Soil Res. 28, 465. https://doi.org/10.1071/SR9900465.
Tormey, D., Donovan, B., 2015. Run Over, Run Up and Run out: A Storm Wave Origin for Fenestral Porosity in Last Interglacial Eolianites of the Bahamas. vol. 47 GSA Abstr. Programs.
Vanoni, V., 1975. Sediment discharge formulas. In: Sedimentation Engineering, pp. 190–229.
Ward, W., 2006. Coastal dunes and strandplains in Southeast Queensland: Sequence and chronology. Aust. J. Earth Sci. 53, 363–373. https://doi.org/10.1080/08120090500507354.
Wasson, R., Hyde, R., 1983. Factors determining desert dune type. Nature 304, 337.
Wessel, B., Huber, M., Wohlfart, C., Marschalk, U., Kosmann, D., Roth, A., 2018. Accuracy assessment of the global TanDEM-X Digital Elevation Model with GPS data. ISPRS Journal of Photogrammetry and Remote Sensing 139, 171–182.
Wilson, A., 1964. Origin of Ice Ages: An Ice Shelf Theory for Pleistocene Glaciation. vol. 3.
https://www.winslow-homer.com/Glass-Windows-Bahamas.html
Wolman, M., Miller, J., 1960. Magnitude and Frequency of forces in Geomorphic Processes. J. Geol. 68, 54–74. https://doi.org/10.1086/626637.
Woodroffe, C., 2002. Coasts: Form, Process, and Evolution. Cambridge University Press, Cambridge; New York.
Yalin, M., 1977. Mechanics of Sediment Transport. Pergamon press, New York, NY.